NASA Technical Memorandum 100504

ANALYSIS OF 7- X 10-FOOT HIGH SPEED WIND TUNNEL SHAFT LOADS IN SUPPORT OF FAN BLADE FAILURE INVESTIGATION

Richard W. Faison

NOVEMBER 1987

National Aeronautics and Space Administration

Langley Research Center
Hampton, Virginia 23665

INTRODUCTION

This analysis was prepared to aid in the failure investigation of the High-Speed 7- x 10-Foot Wind Tunnel. The High-Speed 7- x 10-Foot Wind Tunnel at Langley Research Center, Hampton, Virginia, experienced a catastrophic failure of all 18 Sitka spruce fan blades during operation at 0.8 Mach number on July 9, 1985. The High-Speed Tunnel, a closed-circuit/single-return atmospheric wind tunnel, has been operated since 1945 to support a wide range of subsonic aerodynamic tests and studies. The failed blade set had been in use since 1975. In addition to blade loss, the most significant damage was a bent main drive shaft for a total estimated damage loss of $1.7 million.

An analysis of the natural frequency characteristics as well as loads, reactions, stresses and deflections of the fan drive system resulting from steady-state and dynamic loads due to unbalance was performed. Transient load cases were simulated by step input and ramp input loading functions intended to simulate the loss of one to nine blades (maximum unbalance forces). (Note: The fact that the fan rpm changes and there is a change in inertia with time is not strictly accounted for in this problem but rather, the solution(s) are intended to bound the dynamic response).

ANALYSIS

Math Model:

The 7- x 10-Foot Tunnel drive system is depicted as Figure 1 and consists of an 18-blade fan disk driven by a 14,000 horsepower motor with 14 pole pairs winding giving a top synchronous speed of 514 RPM. The drive system speed is controlled by a motor generator set and liquid rheostat. For this study, the coordinates along the shaft are based on the fan centerline at station 0; the forward bearing at station 33; and the rear bearing at station 191. Pertinent physical characteristics of the drive system are tabulated as Table I and lists weights and inertia of the fan and motor. The analytical programs utilized for this study use a continuous beam approach and the distributive properties are tabulated as Tables II and III for the lateral and torsional studies, respectively. Table II lists the stations along the shaft (x); the distributed mass moment of inertia about a diametric pitch axis; the mass which is the mass per unit length; EI which is the bending stiffness; and ASG which is the shearing stiffness per inch. Similarly, Table III gives the torsional physical characteristics as a function of x (station along the shaft) where ZR is the rotational inertia per inch and JG which is the torsional stiffness per inch.

Governing Equations For Dynamic Response Analysis

The lateral deflection can be represented in modal form solution as:

$$y(x,t) = \sum_{n=1}^{\infty} q_n(t)\ \phi_n(x) \tag{1}$$

The governing differential equation for the generalized coordinate $q_n(t)$ is (assuming initial conditions = 0)

$$\ddot{q}_n(t) + 2\ \zeta_n\ \omega_n\ \dot{q}_n + \omega_n^2\ q_n = \frac{Q_n}{M_n} \tag{2}$$

where

$$Q_n = \sum_{i=1}^{\infty} Pi(t)\ \ \phi_n(x_p) = \text{generalized force}$$

$Pi(t)$ = forcing function on shaft at blades

$\phi_n(x_p)$ = modal deflection at fan blades, station 0

M_n = generalized mass

ω_n = modal frequency, rad/sec

ζ_n = modal dampening (assume .01)

Equation (2) will be solved for two types of generalized force, (a) a step function and (b) a ramp/step function.

The magnitude of the forcing function is dependent upon the number of blades loss. The force per blade is

$$F = mr\omega^2 \tag{3}$$

The following assumptions are made:

18 blades total

Shaft speed = 465 RPM = 48.69 rad/sec

Weight of blade loss = 250 lb/blade

c.g. of blade = 105 inches from centerline

blade spacing = 20°

The force for one blade loss is

$$F = \frac{250}{386} \times 105 \times 48.69^2 = 1.612209\ E05\ lb$$

The force for loss of nine blades loss is

$$F = 1.612E5\ [\sin 90 + 2\ \{\sin 10 + \sin 30 + \sin 50 + \sin 70\}]$$

$$F = 9.283E5\ lb = \text{force of 1/2 blades loss.}$$

Unit Step Function Forcing - The Laplace equation for the unit step forcing with 1/2 the blade loss and initial conditions $q_n(o) = \dot{q}_n(o) = 0$ is:

$$q_n(s) = \frac{9.283E5\ \phi_n(x_p)}{M_n\ S\ [(S + \zeta_n\ \omega_n)^2 + \omega_{nd}^2]} \tag{4}$$

where

$$\omega_{nd} = \omega_n \sqrt{1-\zeta_n^2} \tag{5}$$

is the damped natural frequency. The time domain solution of equation (4) is

$$q_n(t) = \frac{9.283E5\ \phi_n\ (x_p)}{M_n\ \omega_n^2} \left[1 + \frac{e^{-\zeta_n\ \omega_n t}}{\sqrt{1-\zeta_n^2}} \sin\ (\omega_{nd} t - \theta) \right] \tag{6}$$

where

$$\theta = \tan^{-1} \frac{\sqrt{1-\zeta_n^2}}{-\zeta_n} \tag{7}$$

Equation (6) is the generalized coordinate for the nth mode. The moment response due to a step function force applied with zero initial conditions is:

$$M(x,t) = \sum_{n=1}^{\infty} q_n(t)\ \psi_n(x) \tag{8}$$

where $\psi_n(x)$ is the modal moment for the nth mode and M(x,T) is the shaft moment.

The shaft stress is given by:

$$\sigma = \frac{M_c}{I} = \frac{10.18591}{D^3} \quad M(x,t) \tag{9}$$

where D is the shaft diameter at x.

A plot of the first five generalized coordinates is given as Figures 2a to 2e. A plot of the maximum moments along the shaft, that is the maximum values of equation (8) is given as Figure 3. The corresponding maximum shaft shear is given as Figure 4. The shear time history at each side of the bearing is given as Figures 5a and 5b. The moment time history at the bearing is given as Figure 6.

Ramp/step forcing function - The shaft speed of 465 RPM has a period of .129 seconds per revolution. If the forcing peaks in 1/2 of a revolution, the ramp/step function for loss of one-half of the blades can be assumed as follows:

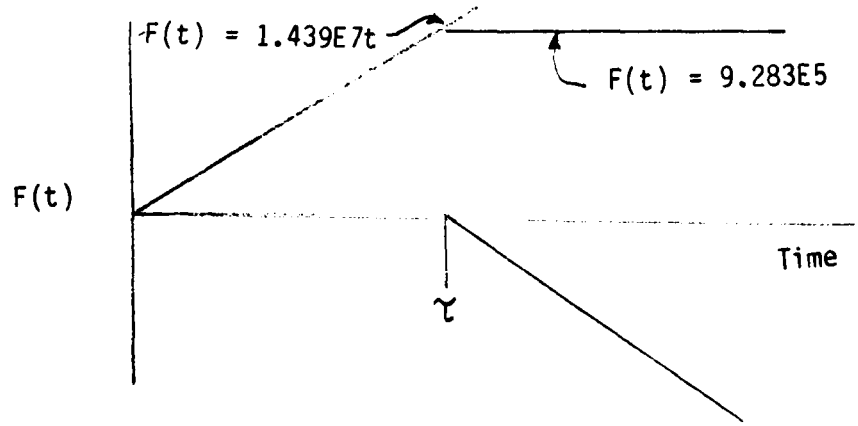

The governing differential equation is:

$$\ddot{q}_n(t) + 2\,\zeta_n\,\omega_n\,\dot{q}_n(t) + \omega_n^2\,q_n(t) = \frac{1.439E7E\ t\ \phi_n\ (x_p)}{M_n}\ [U(t) - U(t-\tau)] \tag{10}$$

The Laplace equation is:

$$q_n(s) = \frac{1.439E7\ \phi_n\ (x_p)\ (1-e^{-\tau s})}{M_n\ S^2\ [(S + \zeta_n\ \omega_n)^2 + \omega_{nd}^2]} \tag{11}$$

$$\text{Let } A_n = \frac{1.439E7\ \phi_n\ (x_p)}{M_n} \tag{12}$$

Then the solution of equation (11) is:

$$q_n(t) = \frac{A_n}{\omega_n^2}\left[t - \frac{e^{-\zeta_n\omega_n t}\ \sin\ \omega_{nd}t}{\omega_{nd}} + \frac{2\zeta_n}{\omega_n}\left(e^{-\zeta_n\ \omega_n t}\ \cos\ \omega_{nd}t - 1\right)\right] \tag{13}$$

For $t \leq \tau$

$$q_n(t) = \frac{A_n}{\omega_n^2}\left[t - \frac{e^{-\zeta_n\omega_n t}\ \sin\ \omega_{nd}t}{\omega_{nd}} + \frac{2\zeta_n}{\omega_n}\left(e^{-\zeta_n\ \omega_n t}\ \cos\ \omega_{nd}t - 1\right)\right]$$

$$- \frac{A_n}{\omega_n^2}\left[(t-\tau) - \frac{e^{-\zeta_n\omega_n(t-\tau)}\ \sin\ \omega_{nd}\ (t-\tau)}{\omega_{nd}}\right.$$

$$\left. + \frac{2\zeta_n}{\omega_n}\left(e^{-\zeta_n\omega_n\ (t-\tau)}\ \cos\ \omega_{nd}(t-\tau) - 1\right)\right] \tag{14}$$

For $t > \tau$

Equations (13) and (14) are the generalized coordinates for the ramp/step input and are plotted on Figures 7a to 7e for generalized coordinates 1 through 5, respectively. Figures 7a-7e are for a rise time to first mode period rates, $\tau_1/\tau_1 = 0.6$. The shaft bearing maximum moment and maximum shear for the ramp/step input is plotted as Figures 8 and 9, respectively. The time history of the shear at each side of the bearing is given as Figure 10a and 10b and the time history of the moment is given as Figure 11.

Load cases studied:

Static loadings of (a) gravity, (b) an unbalance load due to one blade loss, (c) an unbalance load due to nine blades loss were evaluated. The applied loading for the static blade loss was the centrifugal force unbalance only and

did not include the aerodynamic unbalance which is a small effect (adds approximately 10% to all loads). The shaft was assumed to rotate at 465 RPM and the weight of blade loss was 250 pounds at a center of gravity distance of 105 inches from axis of rotation.

Dynamic response studies for nine blades loss were run for a step function and for a ramp/step function where the rise time was varied. Let the rise time be defined as τ_1 and the shaft first mode period as τ; then the ratio τ/τ_1 varied 0, .6, 1., 1.5, 2 for the dynamic runs.

RESULTS AND DISCUSSION

Dynamic Characteristics of Drive System. The lateral and torsional modal analysis of the 7 X 10 tunnel was run on LRC programs LATVIB and TORVIB (refs. 1 and 2), respectively. These programs use a transfer matrix approach for the solution and therefore use a continuous beam description. Table IV lists the lateral and torsional modal frequencies in units of hertz and the generalized masses in units of lb-sec^2/in for the first five modes.

A Campbell diagram for the 7 X 10 tunnel drive is given as Figure 12. All modes are significantly above the 1 per revolution excitation. The first lateral of 15.5 hertz corresponds to the 2 per revolution excitation at the shaft speed of 465 RPM. The 7 X 10 tunnel drive should not, however, have a high 2 per revolution excitation which might exist in an asymmetric shaft design or a shaft drive with self aligning couplings.

A plot of the lateral mode shapes is given as Figure 13 and the torsional mode shapes is given as Figure 14 for the first five modes.

A dynamic response for a step function torque of 1.E6 inch-lb. applied at the fan centerline was accomplished. The generalized coordinates are defined similar to equation (6) of analysis section except torsional frequencies, mass and deflections were used. The maximum torque was calculated and tabulated as Table I. The maximum torque and maximum torsional stress for the step excitation occurs at station 8 which is in the region of the fan keyway.

Steady state response:

The static steady state response was accomplished by a two point boundary value program at LaRC. The forward bearing was simulated by a large spring attached to ground at station 33 and the two boundaries were the free end at the fan and the simply supported rear bearing. The physical properties for the static problem were the same as listed previously for the dynamic studies.

The results for gravity load; 1-blade loss (F = 1.6122ES lb); and 9-blade loss (F = 9.283E5 lb) are given as Figures 15, 16, and 17, respectively. For the tables, y represents the deflection (inches); alpha the slope in units of radians; m the moment in units of inch-pounds; v the shear in units of pounds.

Unbalance force required to deflect blade centerline 0.10 inches (steady state response)

The deflection at the blade centerline (station 0) due to one blade loss (force = 1.6122E5 lbs) was .0588 inch. This would indicate that a static force of (.1/.0589) X 1.6122E5, or a loss of 1.7 blades would be required for wall contact, where 0.10 inch has been assumed to be the blade clearance.

Dynamic response for loss of up to nine blades

The dynamic response for nine-blade loss and having a step function ($\tau/\tau_1 = 0$), where τ_1 = rise time and τ is the first mode period and for a ramp/step function was presented in analysis section. A plot of the maximum moment for the step and ramp/step function was given as Figures 3 and 8, respectively, the latter being presented for the parameter $\tau/\tau_1 = .6$, or the rise time equal to one-half the first mode period. Similar plots were given for the maximum shear in Figures 4 and 9. Figure 6 depicts the resulting moment time history at the forward bearing station 33 and it is evident that the modal participation is almost entirely that of the first mode. The shear history given as Figures 5a and 5b, however, shows significant third mode participation. The dynamic response history for the ramp/step function, Figures 10a, 10b, and 11 show almost entirely first mode participation.

A general statement about the modal participation along the drive shaft is that the modal participation consists of several modes but most of the shaft can be described via the first mode.

The stress in the shaft is given by equation (9) which is

$$\sigma = \frac{10.18591}{D^3} M(x_1 t) \qquad (9)$$

The stress at the forward bearing (x = 33) is obtained with D = 16 inches.

The reaction of the forward bearing is given by the difference between the shear at station x = 33.

The deflection and slope at the forward bearing is given as Table VI for the step and ramp/step function.

As has been mentioned earlier, the dynamic study for the parameter τ/τ_1 was run for τ/τ_1 = 0, .6, 0., 1.5 and 2. Only the plots for $\tau/\tau_1 = .6$ have been included in this report. A tabulation of the results for the complete parametric study has been presented as Table VII. The aerodynamic moment was not included in this study, as has been mentioned earlier. The aerodynamic unbalance would contribute approximately 10 percent the effect of the centrifugal force unbalance. The results of the centrifugal force have been increased by 10 percent for Table VII. The values have been nor malized by their respective static values and presented as Table VIII with a plot shown as Figure 16. On Figure 18 is shown the dynamic factor for a single degree of freedom system. As mentioned earlier, the dynamic response at the forward bearing was mostly the first mode. Had the participation been entirely the first mode, the curves would have been as per the single degree of freedom curve.

The analysis results presented have been for the centrifugal force created by the blade loss. An additional moment load is due to the aerodynamics unbalance due to the blade loss and is approximately 10 percent of moment created by the centrifugal force at the forward bearing. The results presented in Table VII for the moment and stress at the forward bearing account for the aerodynamics unbalance.

A comparison of the calculated bending stresses at the bearing (highest stress point) given in Table VII indicate that partial to total yielding of the shaft would occur (see Table 1-A for strength values). In the case of a circular shaft, the modulus of yield (or rupture) would be 1.6 times the tensile capability. Thus the stress required to form a plastic hinge would be $1.6 \times S_{yield}$ or for fracture $1.6 \times S_{ult}$. Inspection of the drive shaft does show that it is bent and therefore yielded partially so that the solution results in Table VII are believed to bound the loads that the drive system experienced due to blade failure.

Additionally, based on the estimated shear strength properties (see Table 1-B) for the four bearing pedastal tie-down bolts which failed in shear, a reaction at the bearing of approximately 854,000 lbs. would be sufficient to shear the bolts. Comparison of the required reaction load to the calculated loads in Table VII shows that the peak unbalance reaction load for all cases studied is greater than 854,000 lbs.

Dynamic blade loss for .1 inch deflection

The forcing for one-blade loss is 1.6122E5 and for nine-blade loss is 9.283E5. For the step input, the nine-blade loss gave a fan centerline deflection of .8228 inch. Thus

$$\frac{.1\text{" deflection}}{.8228\text{" deflection}} = \frac{\text{FORCE}}{9.283\text{E5}}$$

or FORCE = 1.1728E5 or 70% of one blade

For the ramp/step using $\tau/\tau_1 = 0.6$,

$$\frac{.1\text{" deflection}}{.61752\text{" deflection}} = \frac{\text{FORCE}}{9.283\text{E5}}$$

or FORCE = 1.503E5 or 93% of one blade.

CONCLUSIONS

(1) No instabilities of operational resonances for the drive system were identified.

(2) Upset (unbalance) loads due to blade(s) failure for all cases studied are sufficient to partially or grossly yield the drive shaft, fail the bearing pedestal bolts, and bring the blades into contact with the tunnel shell which would result in almost instantaneous destruction of the blades.

(3) Transient solution results correlate with the damage sustained due to the mishap.

(4) The analysis indicates that the loss of approximately 70% to 93% of the mass of one blade would deflect the centerline of the fan 0.1 inch which is the minimum measured operating gap between the blade tips and the tunnel shell.

RECOMMENDATIONS

(1) Upon completion of repairs, the drive shaft should be instrumented and vibration measurements taken during shakedown.

(2) Permanent drive system monitors should be installed to trip the system offline if excessive vibrations occur.

(3) If the present drive shaft is reused, hardness checks should be made and very thorough inspections completed before installation.

(4) Because of the flexibility of the drive shaft resulting in high sensitivity to unbalance loads, consideration should be given to installing frangible tips on the new blade set and operating with a larger gap between the blade tip and tunnel wall.

REFERENCES

1. Harkins, Barbara; and Geiger, Thomas T.: Computer Program for Natural Modes and Frequencies of a Branched Beam in Transverse Vibration. ER-14441, Martin Company, Baltimore, Maryland. December 1966.

2. Davis, Robert B; and Stephens, Maria V.: A Recurrence Matrix Method for the Analysis of Longitudinal and Torsional Vibrations in Non-Uniform Multibranch Beams with Variable Boundary Conditions. NASA TMX-71973 dated May 6, 1974.

TABLE I

PHYSICAL CHARACTERISTICS OF 7 X 10 TUNNEL

Total drive weight = 79451 lb.

Fan blade and hub weight = 2800 lb.

Motor rotor weight = 30396 lb.

Total drive inertia = 437995 in lb. sec^2

Fan blade and hub inertia = 252787 in lb. sec^2

Motor rotor inertia = 182112 in lb. sec^2

TABLE I-A

SHAFT STRENGTH PROPERTIES

(ESTIMATES FROM HARDNESS CHECKS)

Room Temperature Values

S_{ult} = 95 ksi

S_{yield} = 70 ksi

TABLE I-B

BEARING TIE-DOWN BOLTS ULTIMATE STRENGTH PROPERTIES

(ESTIMATED FROM HARDNESS TESTS)

Tensile Ultimate - 117 ksi

Shear Ultimate - 94 ksi

TABLE II

PHYSICAL CHARACTERISTICS

7X10 TUNNEL LATERAL MODES

X (INCHES)	ZP LB. SEC^2	MASS LB. Sec^2/in^2	EI LB. IN^2	ASG LB.
-17.000	.45865E+00	.65000E-01	.18142E+11	.80950E+09
-11.000	.45865E+00	.65000E-01	.18142E+11	.80950E+09
-11.000	.52664E+04	.31526E+01	.87597E+11	.17788E+10
0.000	.52664E+04	.31526E+01	.90172E+11	.18047E+10
13.000	.52664E+04	.31526E+01	.93293E+11	.18357E+10
13.000	.23586E+01	.14741E+00	.93293E+11	.18357E+10
19.000	.23586E+01	.14741E+00	.93293E+11	.18357E+10
19.000	.39923E+01	.19179E+00	.15791E+12	.23883E+10
24.750	.39923E+01	.19179E+00	.15791E+12	.23883E+10
24.750	.18219E+01	.12956E+00	.72066E+11	.16134E+10
33.000	.18219E+01	.12956E+00	.72066E+11	.16134E+10
33.000	.18219E+01	.12956E+00	.72066E+11	.16134E+10
42.625	.18219E+01	.12956E+00	.72066E+11	.16134E+10
42.625	.39923E+01	.19179E+00	.15791E+12	.23883E+10
50.625	.39923E+01	.19179E+00	.15791E+12	.23883E+10
56.000	.11940E+02	.33167E+00	.47229E+12	.41303E+10
56.000	.17295E+04	.18175E+01	.47229E+12	.41303E+10
82.000	.17295E+04	.18175E+01	.47229E+12	.41303E+10
82.000	.17295E+04	.18175E+01	.46253E+12	.40874E+10
83.000	.17295E+04	.18175E+01	.46253E+12	.40874E+10
96.500	.17295E+04	.18175E+01	.46253E+12	.40874E+10
96.500	.17295E+04	.18175E+01	.45292E+12	.40447E+10
109.500	.17295E+04	.18175E+01	.45292E+12	.40447E+10
109.500	.11450E+02	.32480E+00	.45292E+12	.40447E+10
130.500	.11450E+02	.32460E+00	.45292E+12	.40447E+10
130.500	.11211E+02	.32139E+00	.44346E+12	.40023E+10
148.500	.11211E+02	.32139E+00	.44346E+12	.40023E+10
148.500	.10976E+02	.31800E+00	.43415E+12	.39600E+10
174.500	.10976E+02	.31800E+00	.43415E+12	.39600E+10
180.500	.74627E+00	.82919E-01	.29518E+11	.10326E+10
185.813	.74627E+00	.82919E-01	.29518E+11	.10326E+10
185.813	.35989E+00	.57562E-01	.14235E+11	.71707E+09
191.000	.35989E+00	.57562E-01	.14235E+11	.71707E+09
191.000	.35989E+00	.57562E-01	.14235E+11	.71707E+09
196.188	.35989E+00	.57562E-01	.14235E+11	.71707E+09
196.188	.74627E+00	.82919E-01	.29518E+11	.10326E+10
207.938	.74627E+00	.82919E-01	.29518E+11	.10326E+10
207.938	.35989E+00	.57562E-01	.14235E+11	.71707E+09
217.000	.35989E+00	.57562E-01	.14235E+11	.71707E+09
229.000	.35989E+00	.57562E-01	.14235E+11	.71707E+09

CENTER OF GRAVITY X = 59.31878

TOTAL MASS = 205.83259

S = .12210E+05

TABLE III

PHYSICAL CHARACTERISTICS
FOR TORSIONAL VIBRATIONS

7X10 TUNNEL TORSION MODES

STATION	X (INCHES)	ZR LB. SEC^2	JG LB. IN^2
1= 1	-17.000	.91731E+00	.13763E+11
1= 2	-11.000	.91731E+00	.13763E+11
1= 3	-11.000	.10533E+05	.66453E+11
1= 4	0.000	.10533E+05	.68407E+11
1= 5	13.000	.10533E+05	.70774E+11
1= 6	13.000	.47171E+01	.70774E+11
1= 7	19.000	.47171E+01	.70774E+11
1= 8	19.000	.79846E+01	.11980E+12
1= 9	24.750	.79846E+01	.11980E+12
1= 10	24.750	.30439E+01	.54671E+11
1= 11	42.625	.30439E+01	.54671E+11
1= 12	42.625	.79846E+01	.11980E+12
1= 13	50.625	.79846E+01	.11980E+12
1= 14	56.500	.23881E+02	.35829E+12
1= 15	56.500	.34590E+04	.35829E+12
1= 16	82.000	.34590E+04	.35829E+12
1= 17	82.000	.34590E+04	.35089E+12
1= 18	83.000	.34590E+04	.35089E+12
1= 19	96.500	.34590E+04	.35089E+12
1= 20	96.500	.34590E+04	.34359E+12
1= 21	109.500	.34590E+04	.34359E+12
1= 22	109.500	.22901E+02	.34359E+12
1= 23	130.500	.22901E+02	.34359E+12
1= 24	130.500	.22423E+02	.33642E+12
1= 25	148.500	.22423E+02	.33642E+12
1= 26	148.500	.21952E+02	.32935E+12
1= 27	174.500	.21952E+02	.32935E+12
1= 28	180.500	.14925E+01	.22393E+11
1= 29	185.813	.14925E+01	.22393E+11
1= 30	185.813	.71978E+00	.10799E+11
1= 31	196.188	.71978E+00	.10799E+11
1= 32	196.188	.14925E+01	.22393E+11
1= 33	207.938	.14925E+01	.22393E+11
1= 34	207.938	.71978E+00	.10799E+11
1= 35	229.000	.71978E+00	.10799E+11

CENTER OF ROTART INERTIA = 35.86546

TOTAL ROTARY INERTIA = .4379950E+06

TABLE IV

MODE	LATERAL FREQUENCY (Hz)	LATERAL GENERALIZED MASS	TORSIONAL FREQUENCY (Hz)	TORSIONAL GENERALIZED MASS
1	15.517	.9477058E2	18.015	.1865477E6
2	41.505	.9890384E2	55.555	.1336389E6
3	71.782	.1650873E3	96.238	.8230074E5
4	116.054	.7522273E1	104.498	.1312093E6
5	131.51	.1084724E2	150.1341	.9236134E5

TABLE V
MAXIMUM TORSIONAL RESPONSE DUE TO STEP FUNCTIONS

TRANSONIC DYNAMIC TUNNEL TORSIONAL ANALYSIS

GENERALIZED COORDINATE 1 = -.1952220E-03
GENERALIZED COORDINATE 2 = .2412180E-05
GENERALIZED COORDINATE 3 = .5678592E-05
GENERALIZED COORDINATE 4 = -.1632897E-04
GENERALIZED COORDINATE 5 = .3090223E-05

X	TIME	MAX TORQUE
-17.000	0.0000000	0.
-15.000	.0275799	.1297493E+02
-13.000	.0275799	.2594861E+02
-11.000	.0275799	.3891980E+02
-11.000	.0275799	.3891980E+02
-9.000	.0275799	.1489550E+06
-7.000	.0275799	.2640315E+06
-5.000	.0275799	.3208670E+06
-3.000	.0298782	.3174364E+06
-1.000	.0298782	.3222724E+06
0.000	.0298782	.3074378E+06
2.000	.0229832	.3457431E+06
4.000	.0229832	.4307049E+06
6.000	.0252815	.4991700E+06
8.000	.0252815	.5269372E+06
10.000	.0252815	.4996211E+06
12.000	.0252815	.4299358E+06
13.000	.0275799	.4414643E+06
13.000	.0275799	.4414643E+06
15.000	.0275799	.4414964E+06
17.000	.0275799	.4415249E+06
19.000	.0275799	.4415495E+06
19.000	.0275799	.4415495E+06
21.000	.0275799	.4415863E+06
23.000	.0275799	.4416194E+06
24.750	.0275799	.4416453E+06
24.750	.0275799	.4416453E+06
26.750	.0275799	.4416562E+06
28.750	.0275799	.4416633E+06
30.750	.0275799	.4416668E+06
32.750	.0275799	.4416665E+06
34.750	.0275799	.4416625E+06
36.750	.0275799	.4416548E+06
38.750	.0275799	.4416433E+06
40.750	.0275799	.4416281E+06
42.625	.0275799	.4416105E+06
42.625	.0275799	.4416105E+06
44.625	.0275799	.4415637E+06
46.625	.0275799	.4415132E+06
48.625	.0275799	.4414589E+06
50.625	.0275799	.4414009E+06
52.625	.0275799	.4413177E+06
54.625	.0275799	.4411886E+06
56.500	.0275799	.4410244E+06
56.500	.0275799	.4410244E+06
58.500	.0298782	.4128767E+06
60.500	.0298782	.3985652E+06

X	TIME	MAX TORQUE
62.500	.0298782	.3836711E+06
64.500	.0827396	.3734404E+06
66.500	.0827396	.3711408E+06
68.500	.0827396	.3679684E+06
70.500	.0827396	.3637714E+06
72.500	.0321765	.3584933E+06
74.500	.0321765	.3561951E+06
76.500	.0321765	.3521830E+06
78.500	.0321765	.3463092E+06
80.500	.0321765	.3384527E+06
82.000	.0321765	.3311981E+06
82.000	.0321765	.3311981E+06
83.000	.0321765	.3256933E+06
85.000	.0321765	.3130450E+06
87.000	.0321765	.2981845E+06
89.000	.0321765	.2811255E+06
91.000	.0321765	.2619162E+06
93.000	.0321765	.2406390E+06
95.000	.0321765	.2174091E+06
96.500	.0321765	.1988007E+06
96.500	.0321765	.1988007E+06
98.500	.0321765	.1725078E+06
100.500	.0321765	.1447023E+06
102.500	.0321765	.1156095E+06
104.500	.0321765	.8547610E+05
106.500	.0321765	.5456619E+05
108.500	.0321765	.2315684E+05
109.500	.0321765	.7371643E+04
109.500	.0321765	.7371643E+04
111.500	.0321765	.7162285E+04
113.500	.0321765	.6952486E+04
115.500	.0321765	.6742259E+04
117.500	.0321765	.6531617E+04
119.500	.0321765	.6320572E+04
121.500	.0321765	.6109138E+04
123.500	.0321765	.5897327E+04
125.500	.0321765	.5685151E+04
127.500	.0321765	.5472625E+04
129.500	.0321765	.5259761E+04
130.500	.0321765	.5153207E+04
130.500	.0321765	.5153207E+04
132.500	.0321765	.4944312E+04
134.500	.0321765	.4735112E+04
136.500	.0321765	.4525619E+04
138.500	.0321765	.4315846E+04
140.500	.0321765	.4105805E+04
142.500	.0321765	.3895511E+04

TABLE V (CONT'D)

X	TIME	MAX TORQUE
144.500	.0321765	.3684975E+04
146.500	.0321765	.3474210E+04
148.500	.0321765	.3263230E+04
148.500	.0321765	.3263230E+04
150.500	.0321765	.3056480E+04
152.500	.0321765	.2849540E+04
154.500	.0321765	.2642423E+04
156.500	.0321765	.2435143E+04
158.500	.0321765	.2227711E+04
160.500	.0321765	.2020140E+04
162.500	.0321765	.1812445E+04
164.500	.0321765	.1604636E+04
166.500	.0321765	.1396728E+04
168.500	.0321765	.1188733E+04
170.500	.0321765	.9806641E+03
172.500	.0321765	.7725341E+03
174.500	.0321765	.5643560E+03
176.500	.0321765	.3884883E+03
178.500	.0321765	.2772880E+03
180.500	.0321765	.2307749E+03
182.500	.0321765	.2165995E+03
184.500	.0321765	.2024106E+03
185.813	.0321765	.1930922E+03
185.813	.0321765	.1930922E+03
187.813	.0321765	.1862364E+03
189.813	.0321765	.1793690E+03
191.813	.0321765	.1724904E+03
193.813	.0321765	.1656008E+03
195.813	.0321765	.1587009E+03
196.188	.0321765	.1574061E+03
196.188	.0321765	.1574061E+03
198.188	.0321765	.1430793E+03
200.188	.0321765	.1287435E+03
202.188	.0321765	.1143996E+03
204.188	.0321765	.1000485E+03
206.188	.0321765	.8569116E+02
207.938	.0321765	.7312404E+02
207.938	.0321765	.7312404E+02
209.938	.0321765	.6619445E+02
211.938	.0321765	.5926069E+02
213.938	.0321765	.5232320E+02
215.938	.0321765	.4538241E+02
217.938	.0321765	.3843877E+02
219.938	.0321765	.3149271E+02
221.938	.0321765	.2454467E+02
223.938	.0321765	.1759508E+02
225.938	.0321765	.1064438E+02
227.938	.0321765	.3693008E+01
227.000	0.0000000	.1747663E-05

TABLE VI

DEFLECTION AND SLOPE AT FAN CENTERLINE

STEP FUNCTION

Mode	$q_n(t = .033592)$	$\Phi_n(x_p = 0)$	$\Psi_n(x_p = 0)$	$y_n = q_n\Phi_n$	$yn = q_n\Psi_n$
1	1.278262	.60162	-.022707	.7690279	- .02902549
2	- .01081068	-.044972	-.0083563	8.14299-4	1.513058-4
3	.04782744	.98205	.016846	4.696893-2	8.05701-4
4	- .002432855	-.023794	-.0016474	5.788735-5	4.007885-6
5	.03610952	.16984	.0061097	6.132671-3	2.206122-4
				y_n = .8228	yn = -2.7849-2
					= -1.59566 deg.

RAMP/STEP FUNCTION t = .0387

Mode	$q_n(t = .0387)$	$\Phi_n(x_p = 0)$	$\Psi_n(x_p = 0)$	$y_n = q_n\Phi_n$	$yn = q_n\psi_n$
1	.97	.60162	-.022707	.583571	- .022026
2	- .0076	-.044972	-.0083563	3.41787-4	6.351-5
3	.0302	.98205	.016846	.02966	5.0875-4
4	- .00615	-.023794	-.0016474	1.4633-4	1.01315-5
5	.0226	.16984	.0061097	3.83838-3	1.3808-4
				y_n = .617519	yn = -2.13-2
					= -1.2207 deg.

TABLE VII

9 BLADE LOSS
DYNAMIC RESPONSES AS A FUNCTION
OF RISE TIME

τ/τ_1	BEARING MOMENT (SHAFT) (IN. LB.)	BEARING STRESS (SHAFT) (KSI)	BEARING REACTION (LB)	FAN ℄ SLOPE (DEGREE)	FAN ℄ DEFLECTION INCH
0	6.78E7	168.5	2.15E6	-1.756	.905
0.6	4.97E7	123.8	1.41E6	-1.342	.679
1.0	3.59E7	88.1	1.22E6	- .893	.470
1.5	4.11E7	102.2	1.28E6	-1.073	.552
2.0	3.56E7	88.6	1.20E6	-9.01	.516
STATIC	3.42E7	85.0	1.28E6	- .761	.384

TABLE VIII

NORMALIZED DYNAMIC RESPONSES AS A FUNCTION OF RISE TIME

τ/τ_1	BEARING MOMENT (SHAFT)	BEARING STRESS (SHAFT	BEARING REACTION	FAN ℄ SLOPE	FAN ℄ DEFLECTION
0	1.982	1.982	1.685	2.306	2.354
0.6	1.456	1.456	1.106	1.763	1.767
1.0	1.048	1.036	.96	1.173	1.223
1.5	1.203	1.202	1.0	1.409	1.436
2.0	1.04	1.04	.942	1.884	1.342
STATIC	1.0	1.0	1.0	1.0	1.0

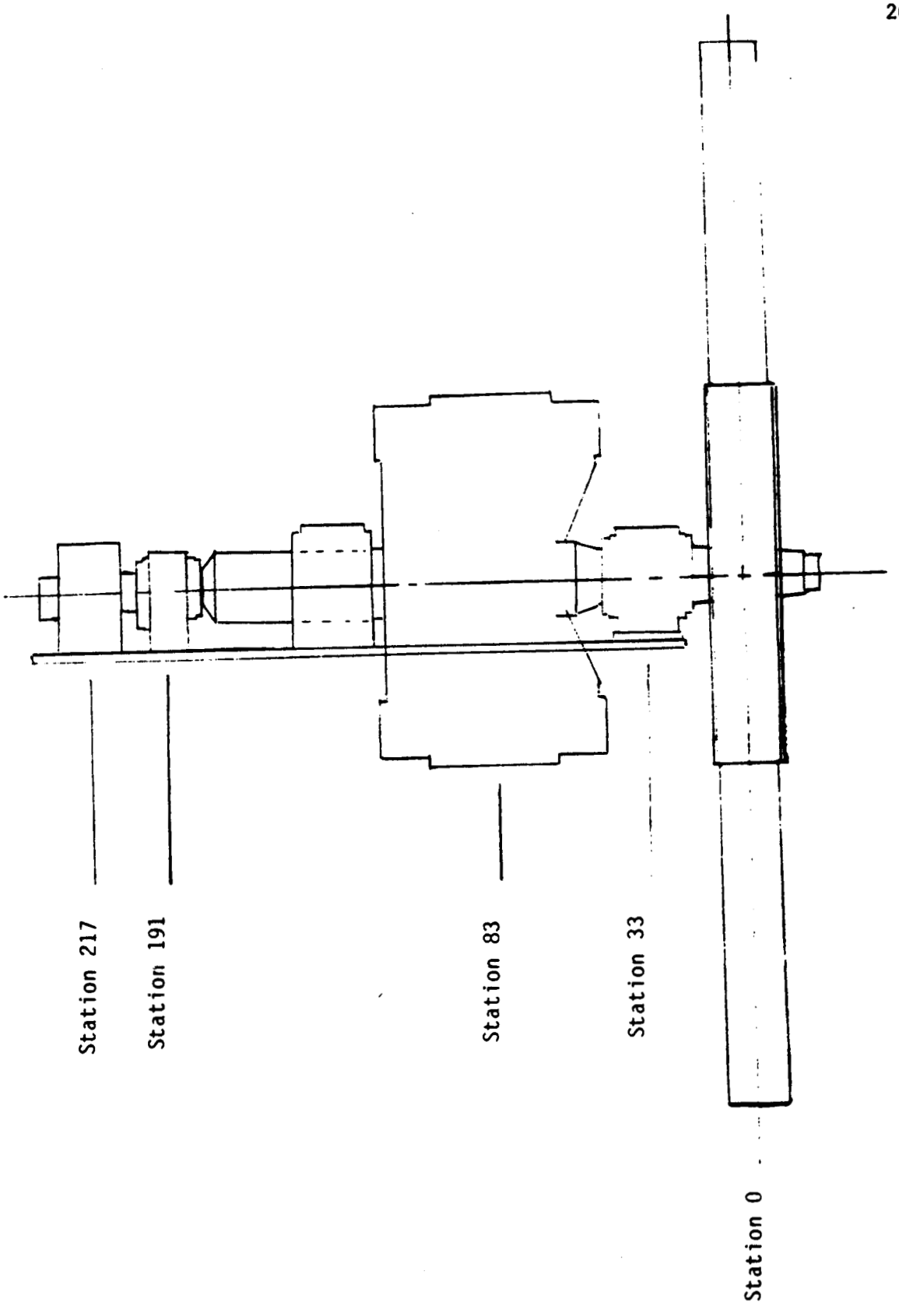

Figure 1. - 7 X 10 drive system

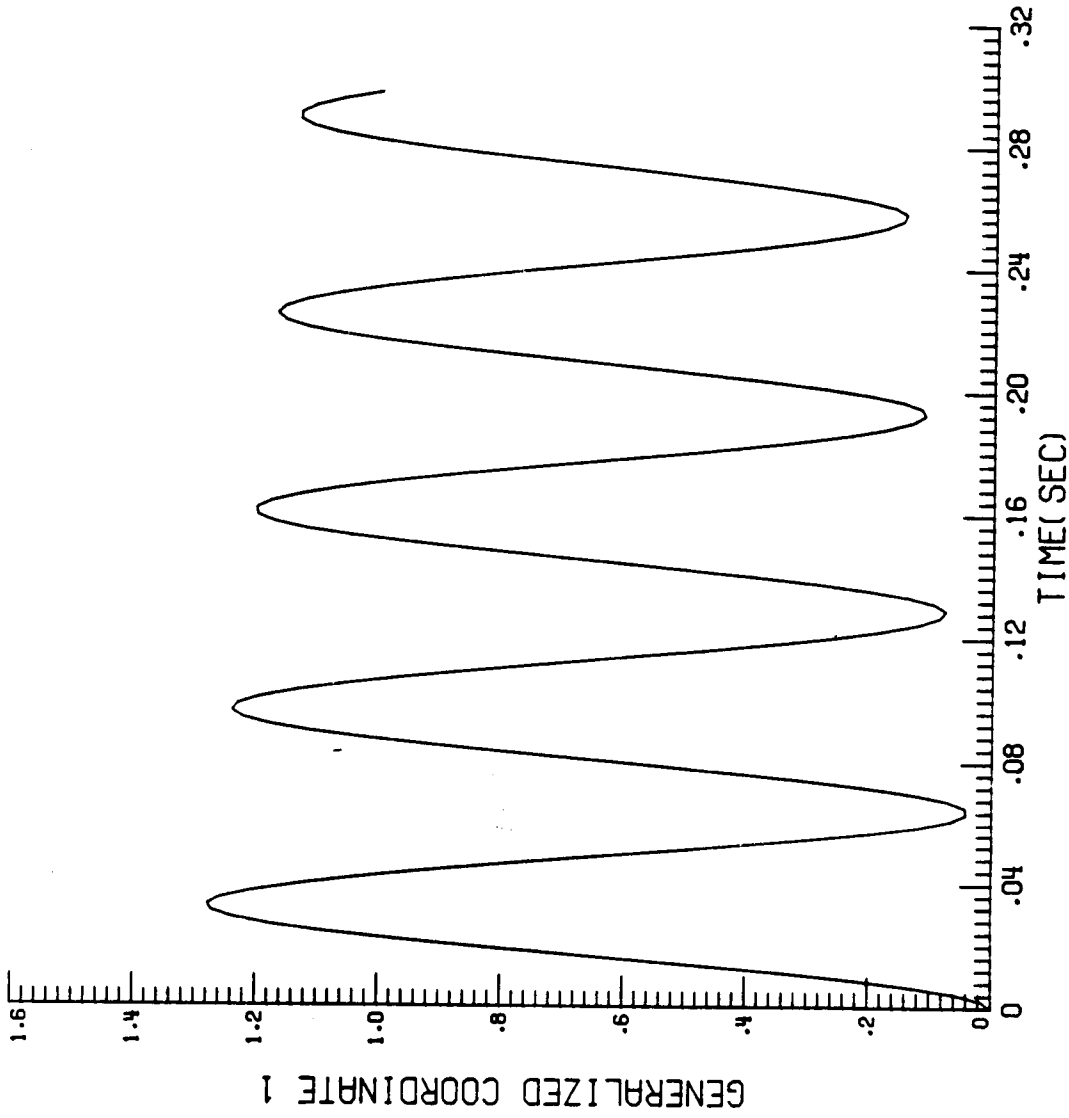

Figure 2a. - Mode 1 Generalized Coordinate for Step Function.

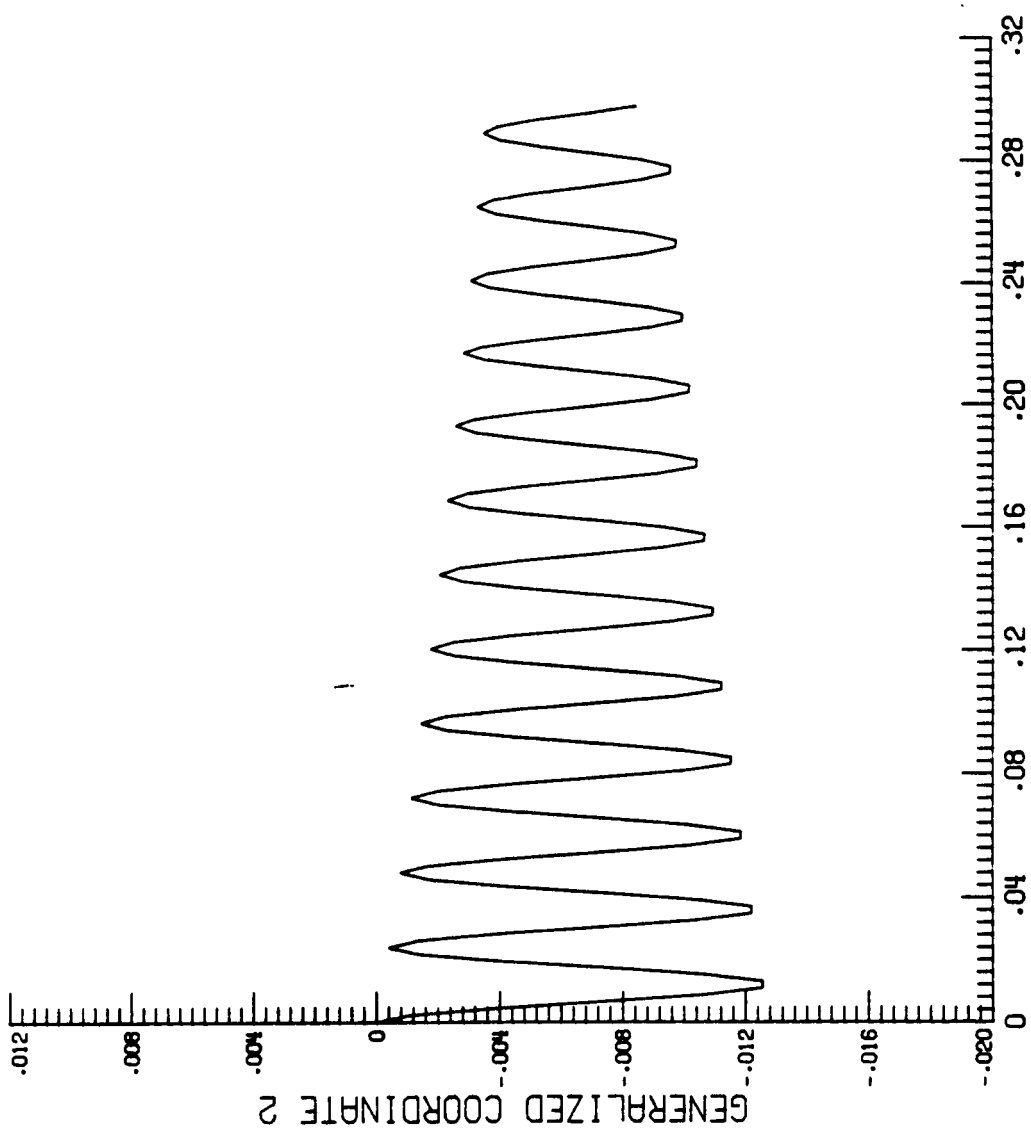

Figure 2b. - Mode 2 Generalized Coordinate for Step Function.

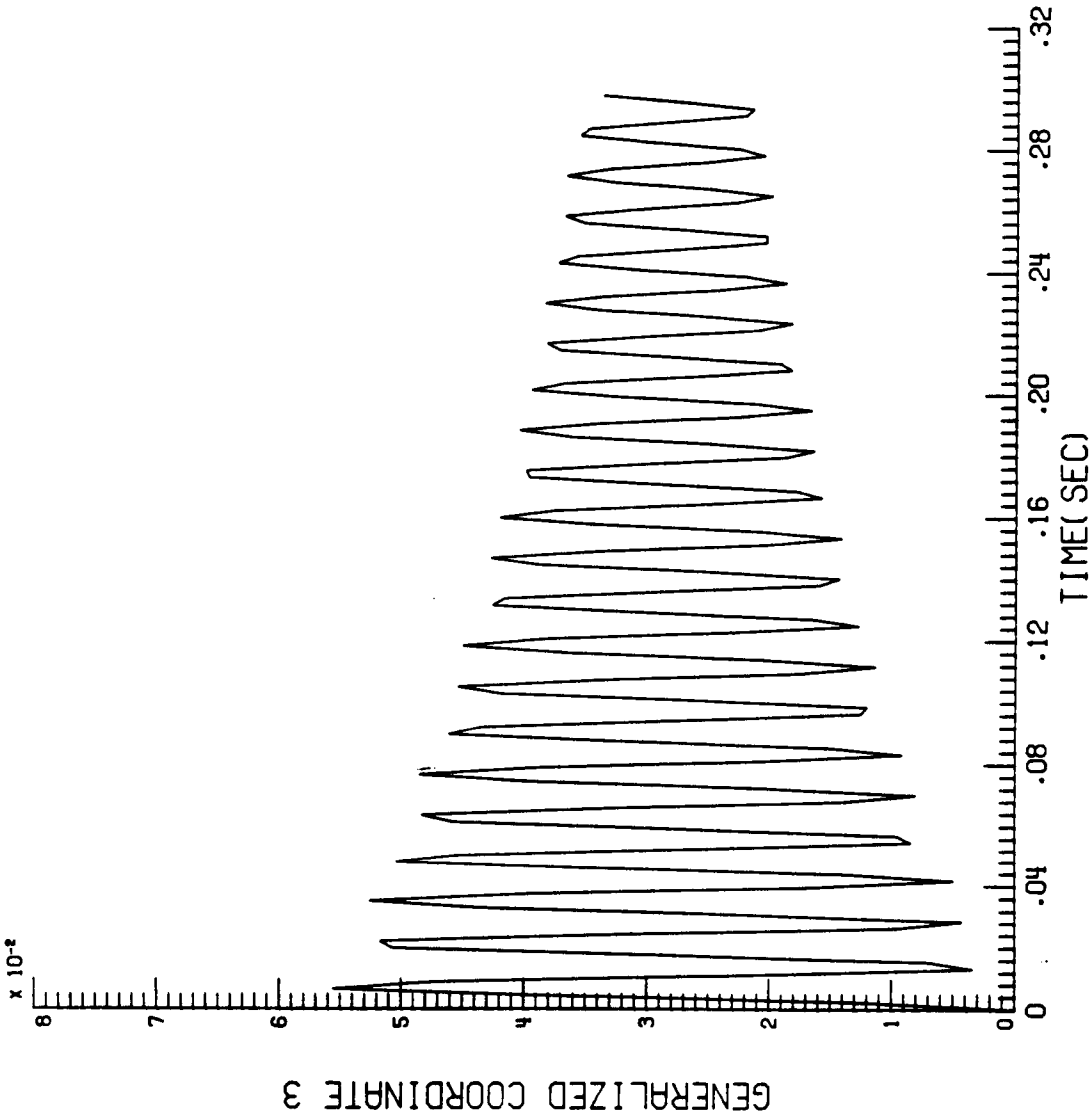

Figure 2c. - Mode 3 Generalized Coordinate for Step Function.

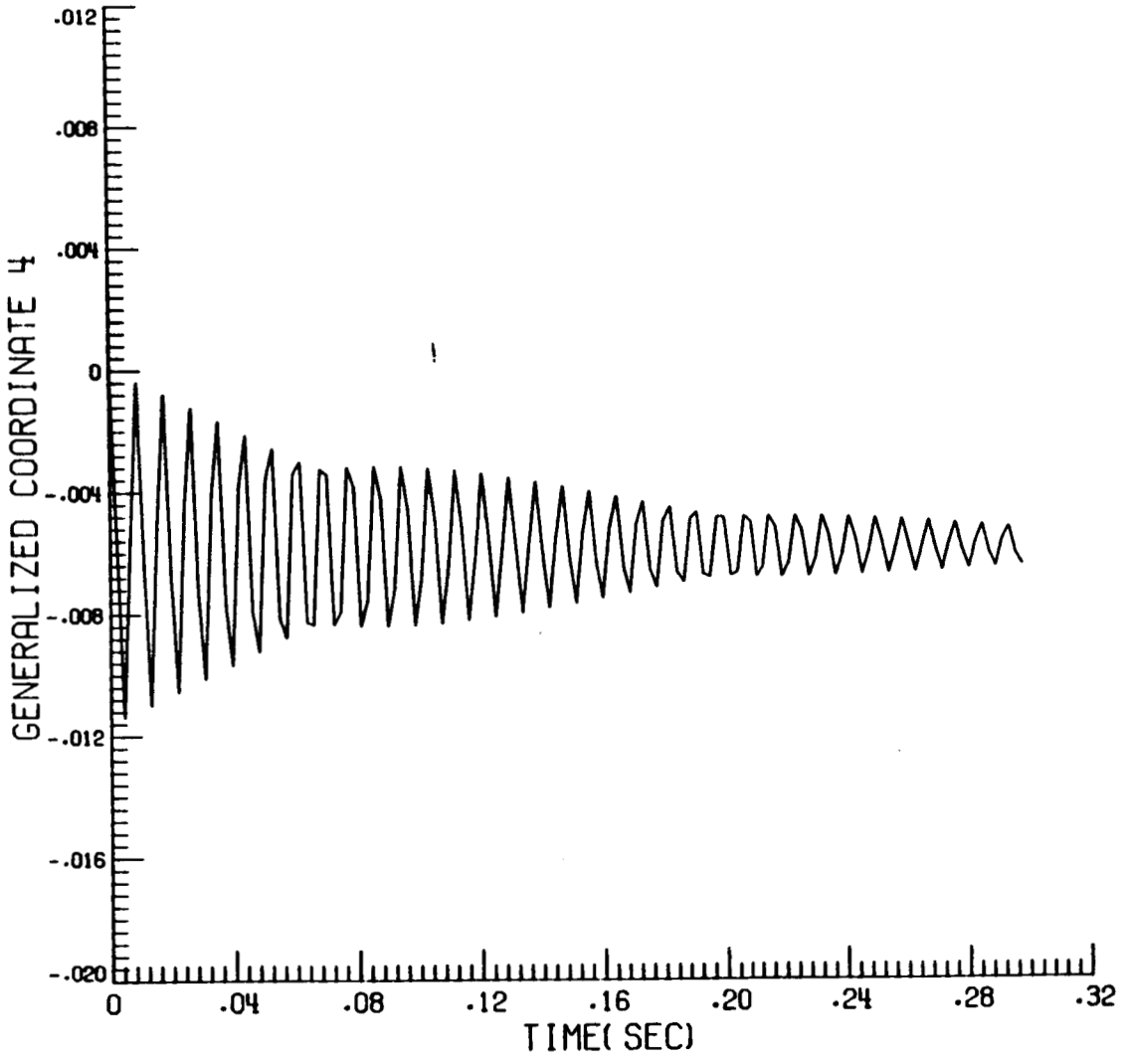

Figure 2d. - Mode 4 Generalized Coordinate for Step Function.

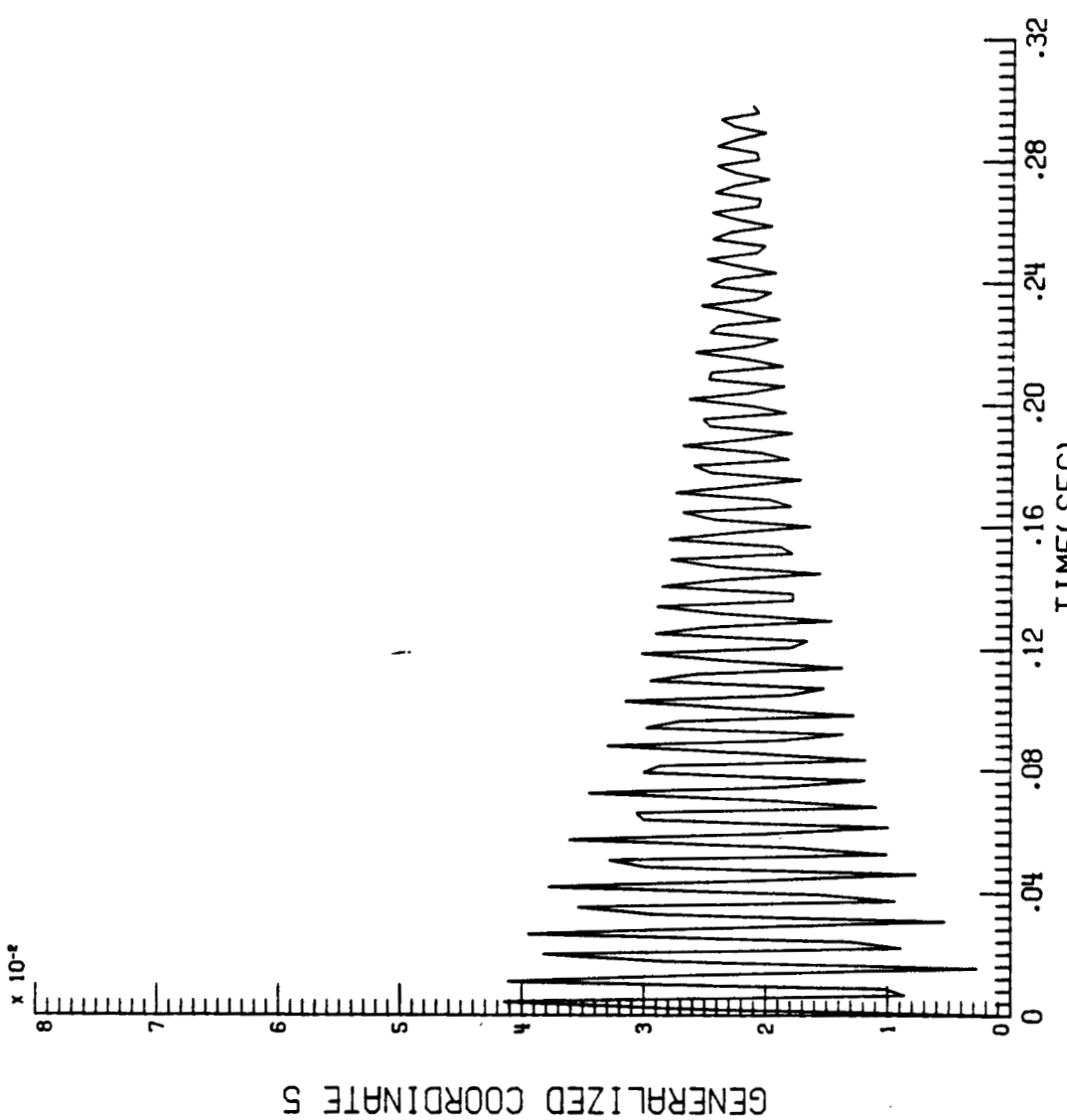

Figure 2e. - Mode 5 Generalized Coordinate for Step Function.

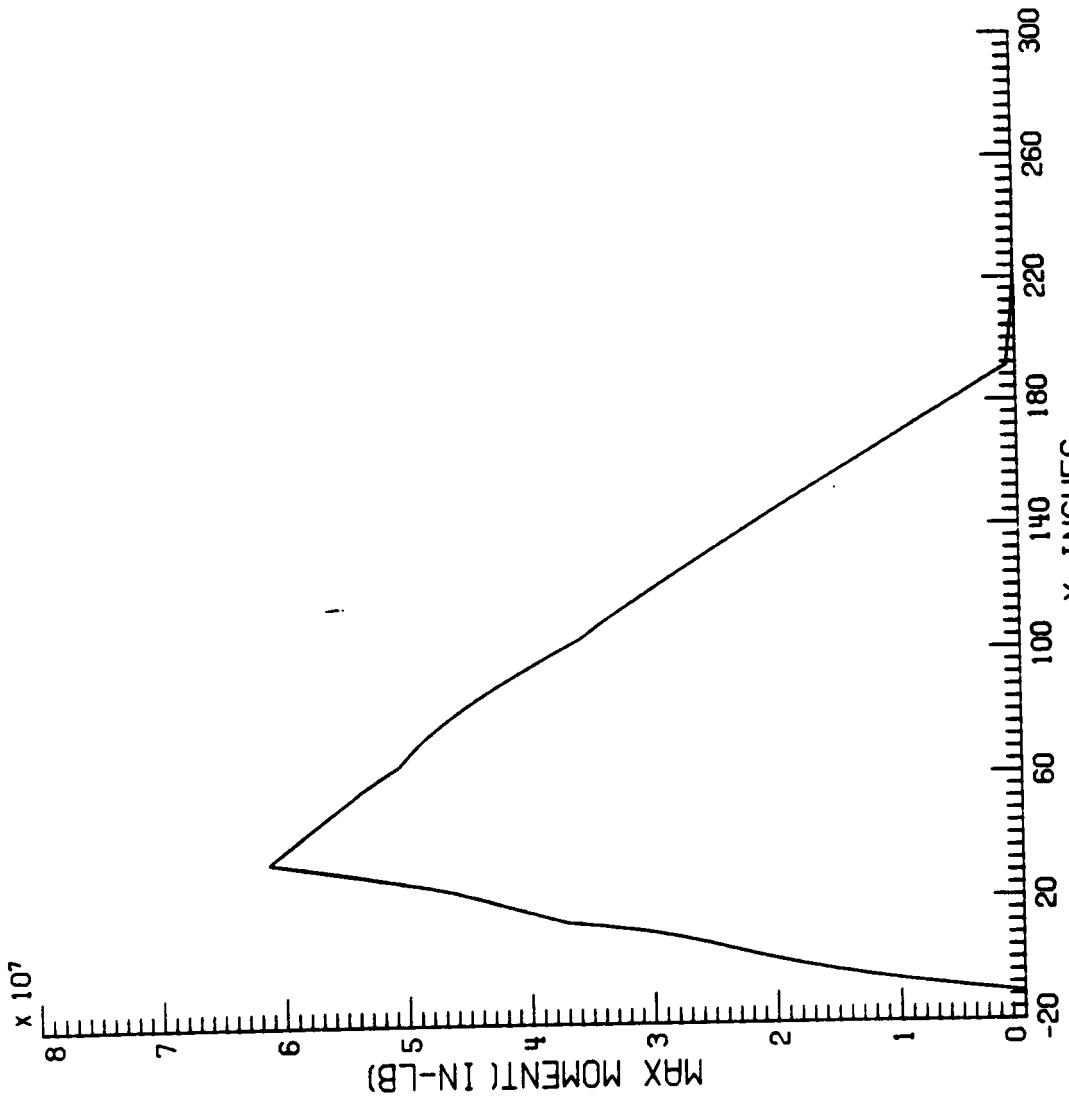

Figure 3. - Maximum Moment at Forward Bearing for Step Function.

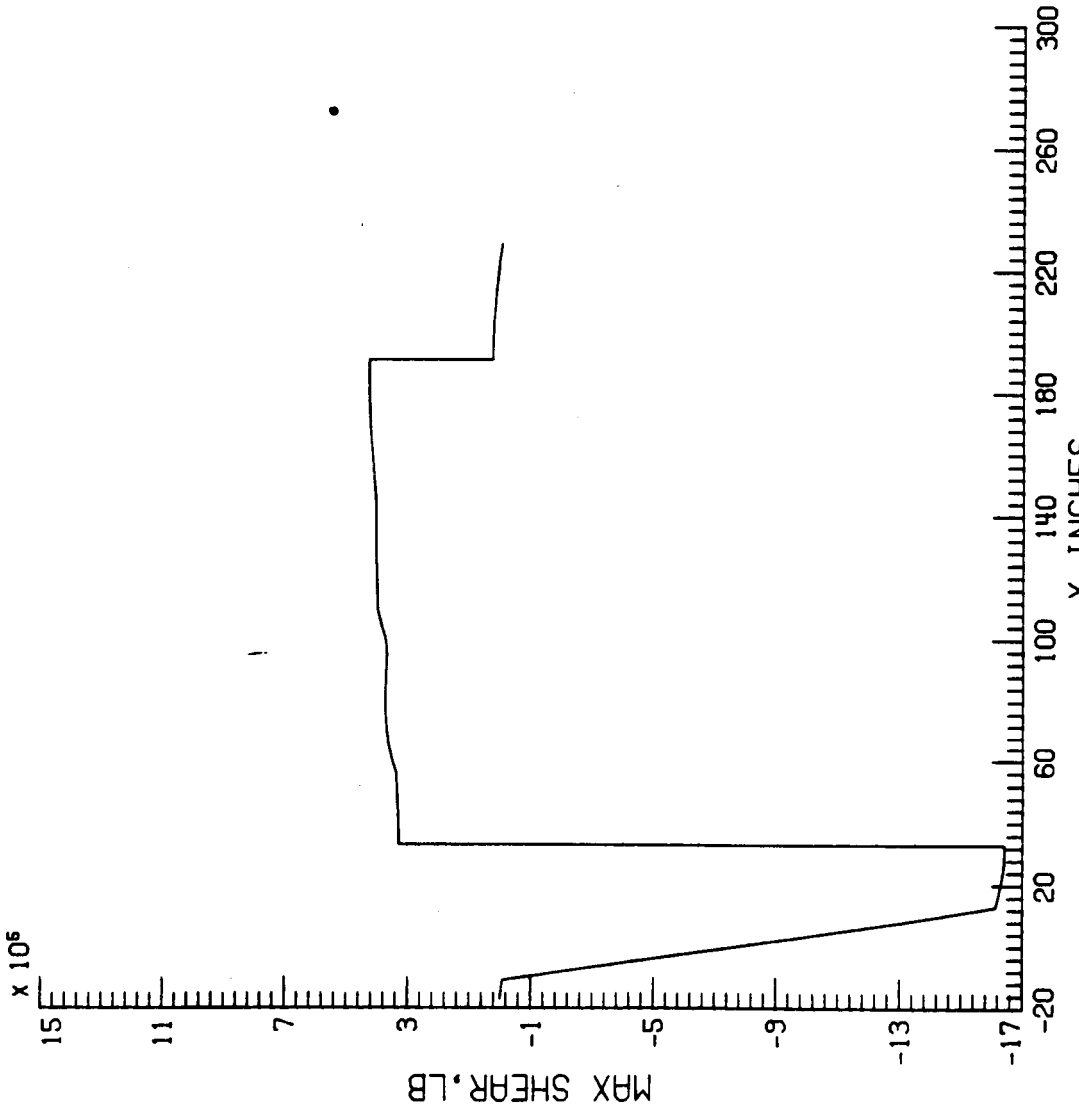

Figure 4. - Maximum Shear for Step Function at Forward Bearing.

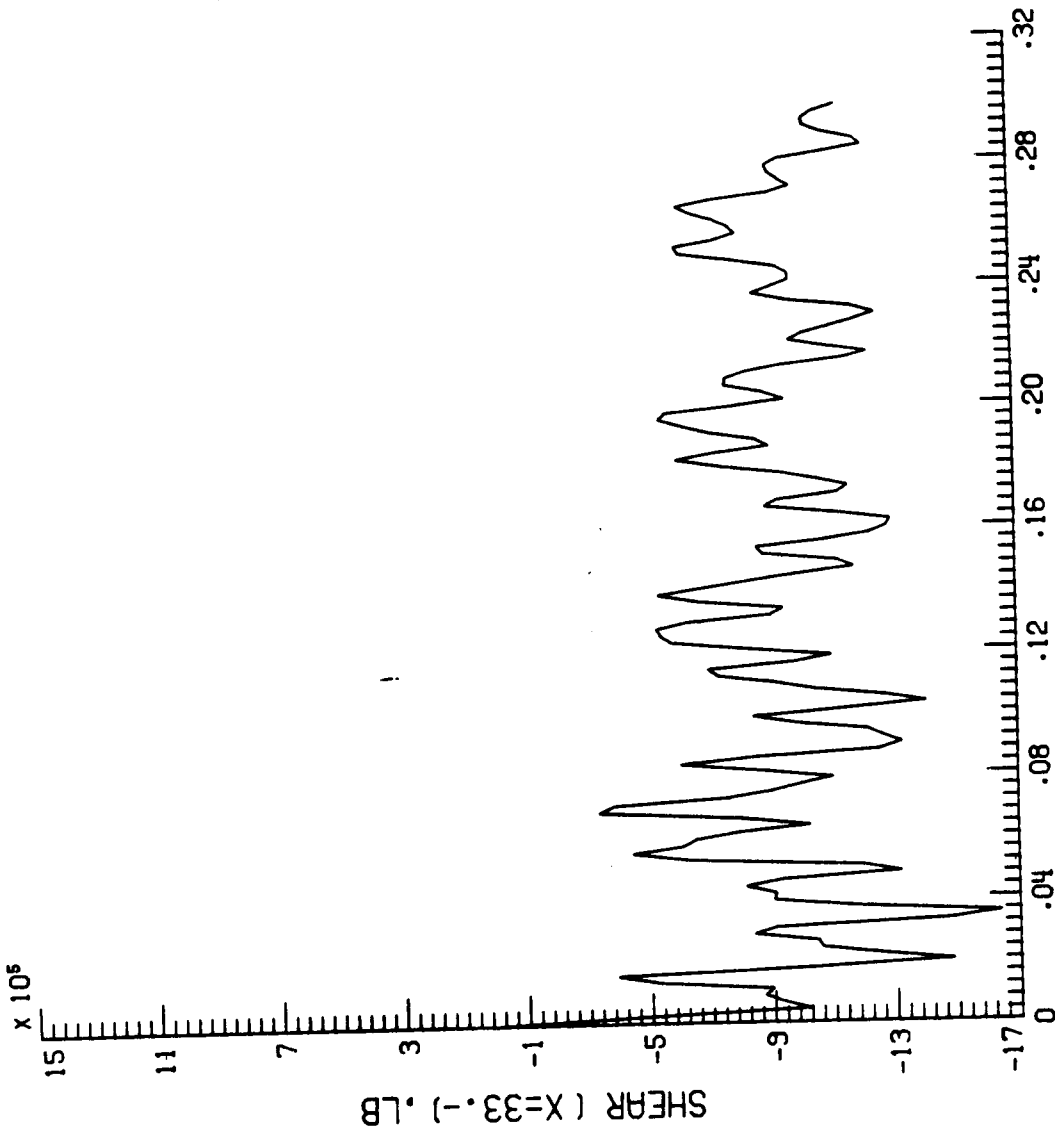

Figure 5a. - Step Function Shear at Forward Bearing.

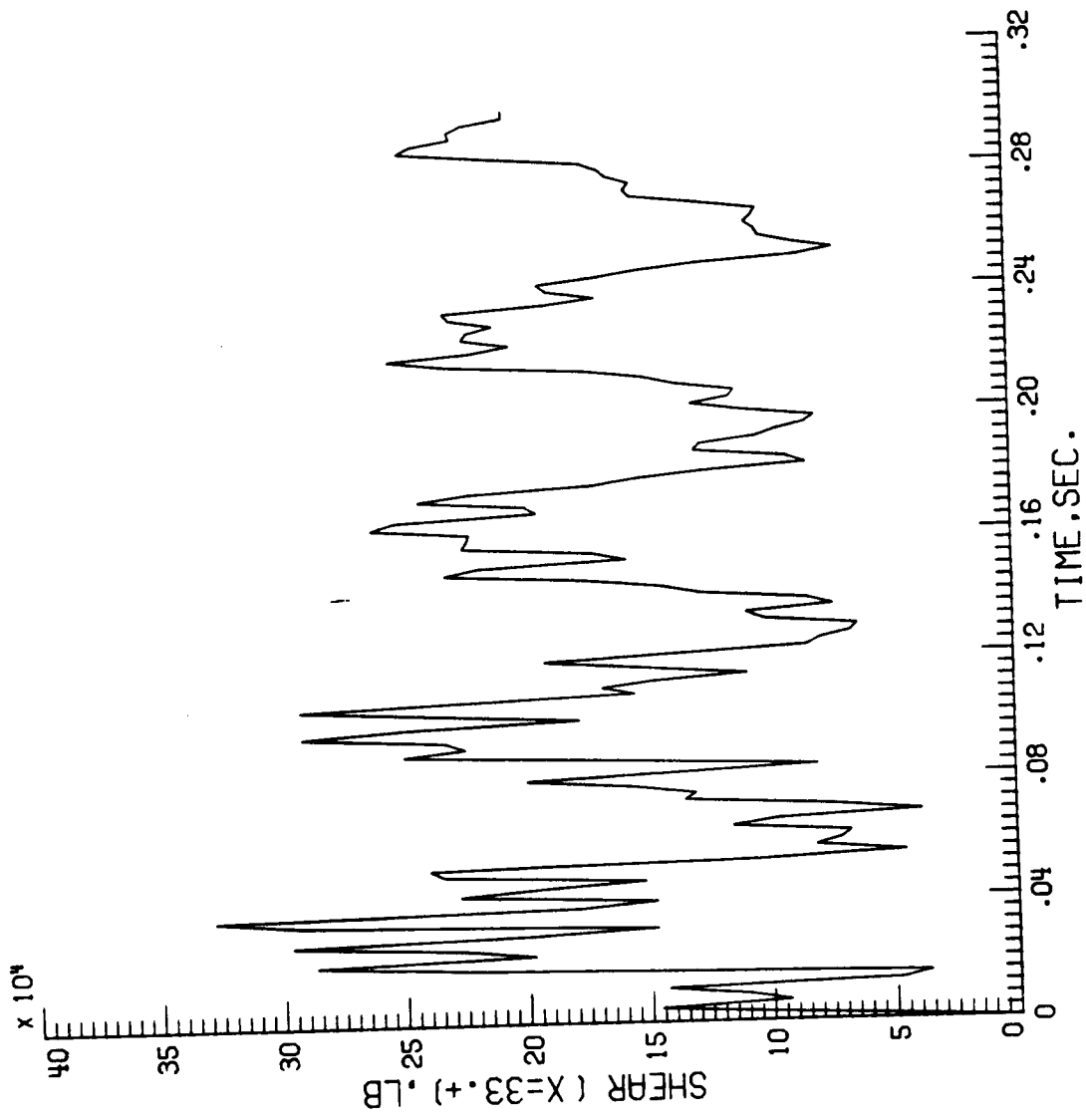

Figure 5b. - Step Function Shear at Forward Bearing.

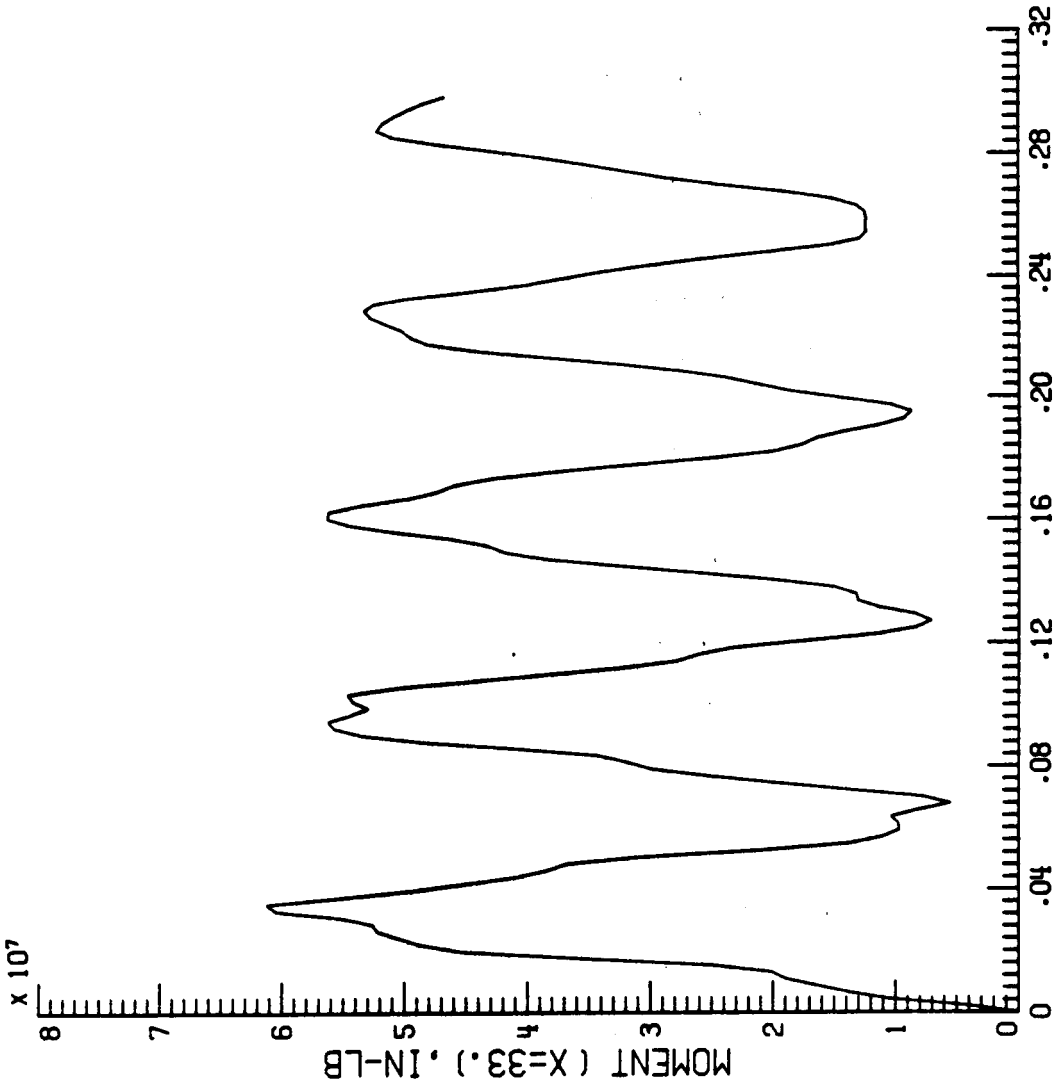

Figure 6. - Step Function Moment at Forward Bearing.

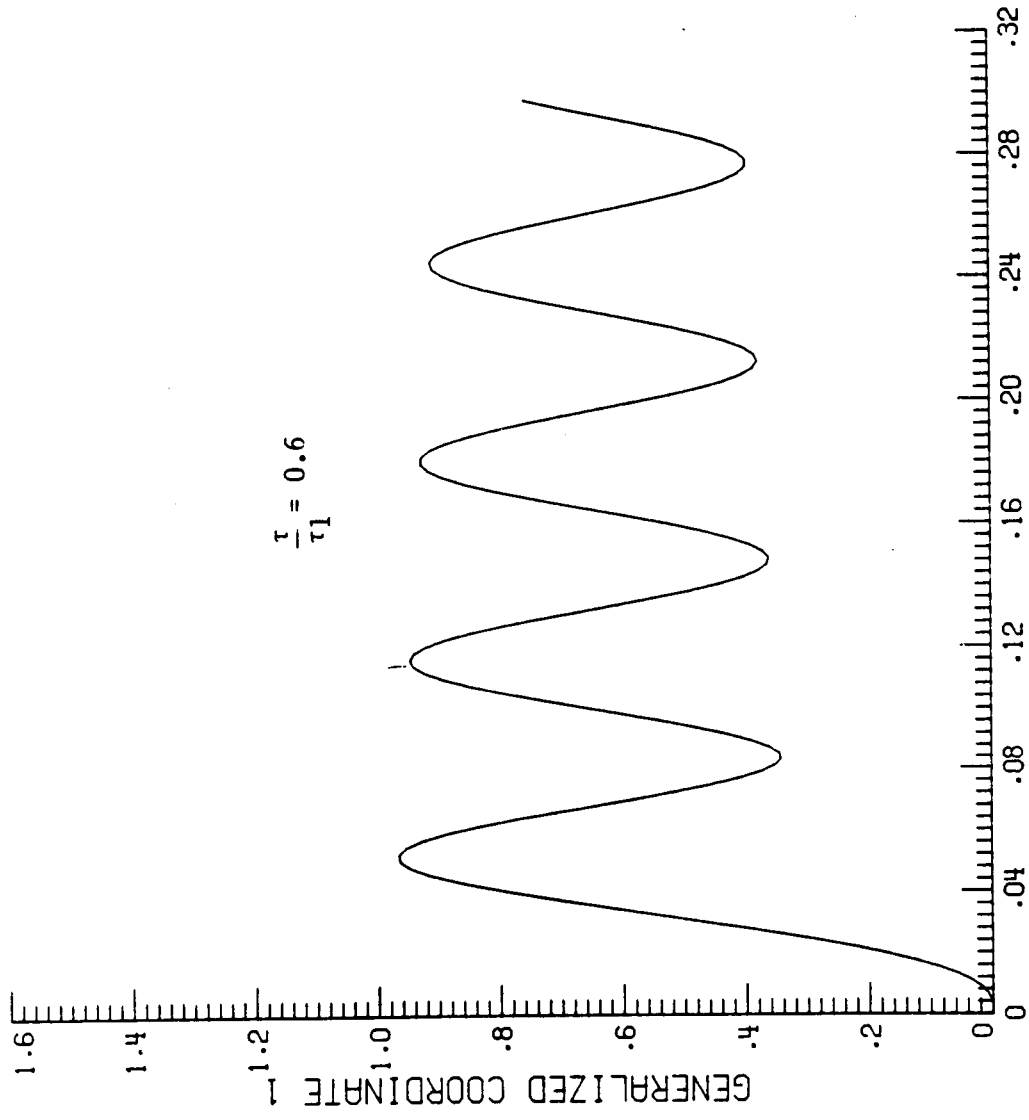

Figure 7a. - Mode 1 Generalized Coordinate for Ramp/Step Function.

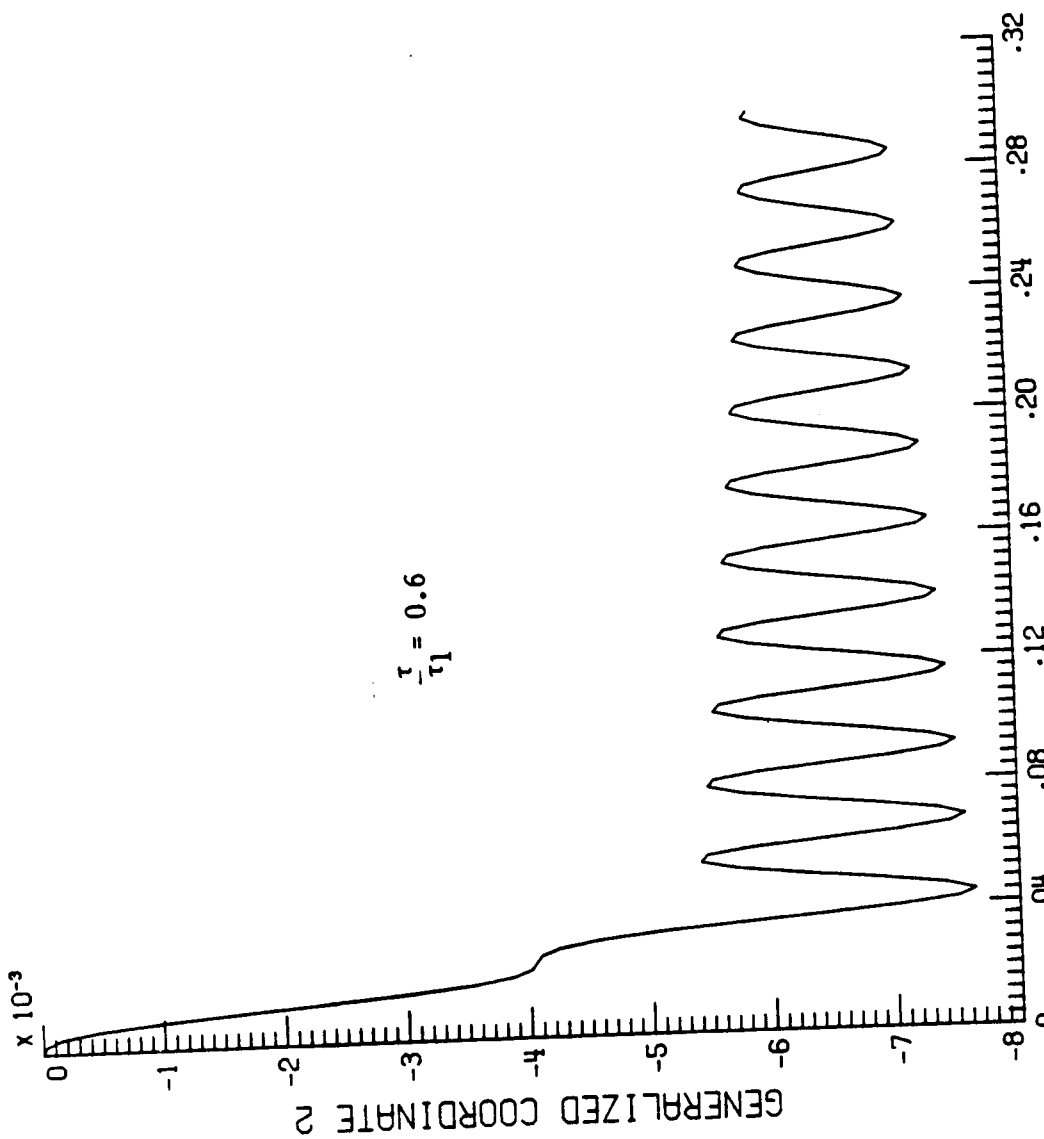

Figure 7b. - Mode 2 Generalized Coordinate for Ramp/Step Function.

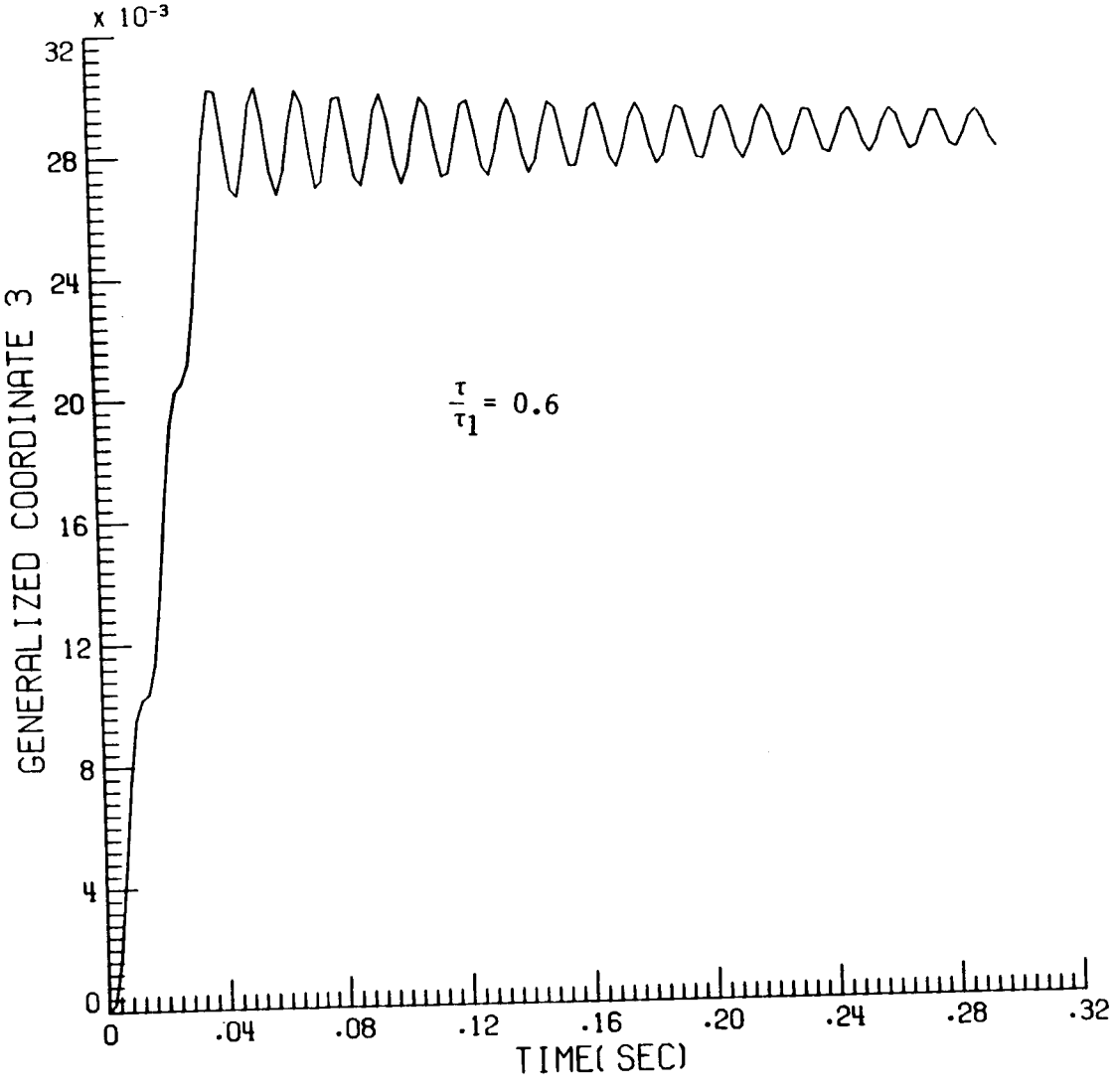

Figure 7c. - Mode 3 Generalized Coordinate for Ramp/Step Function.

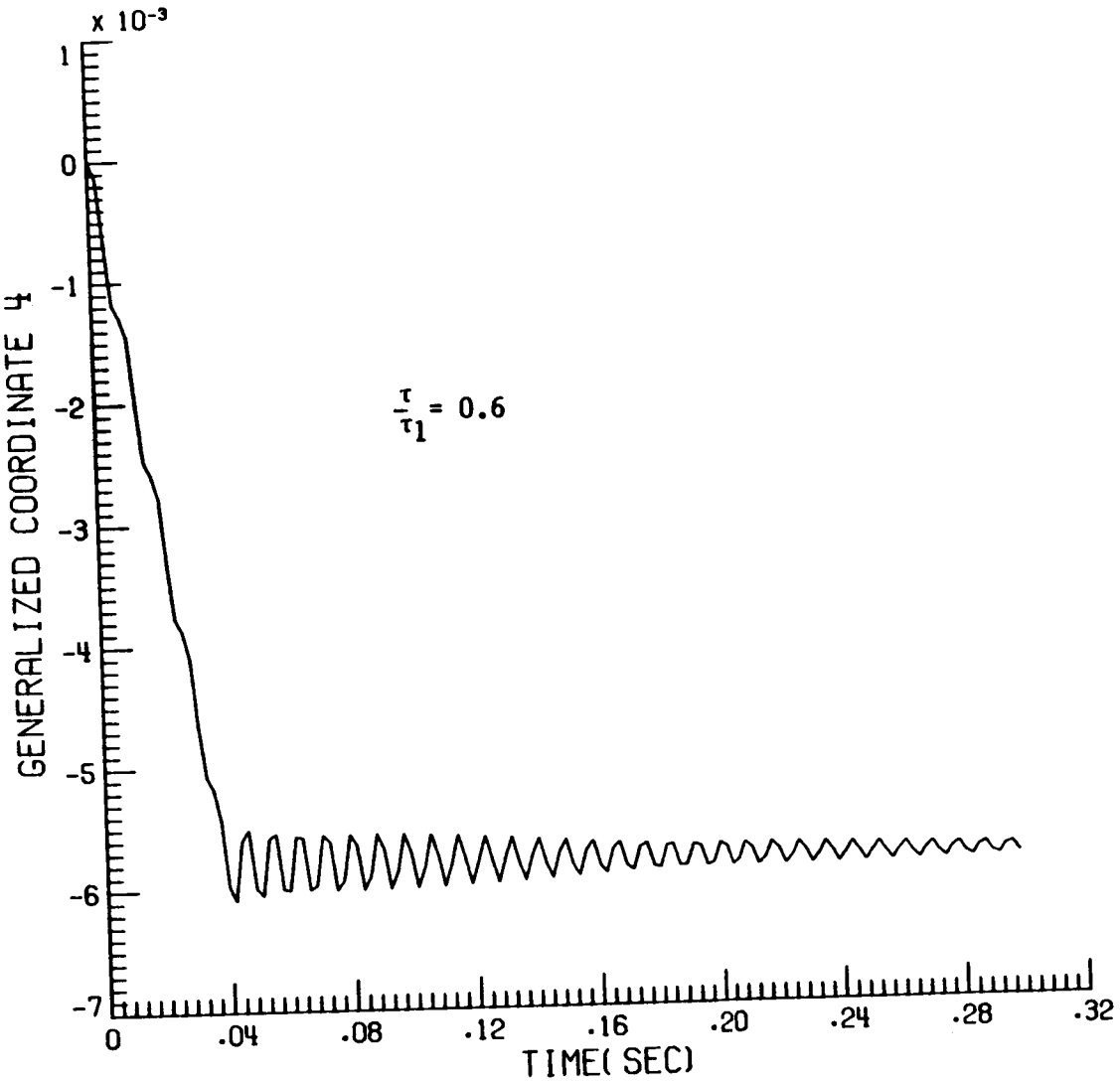

Figure 7d. - Mode 4 Generalized Coordinate for Ramp/Step Function.

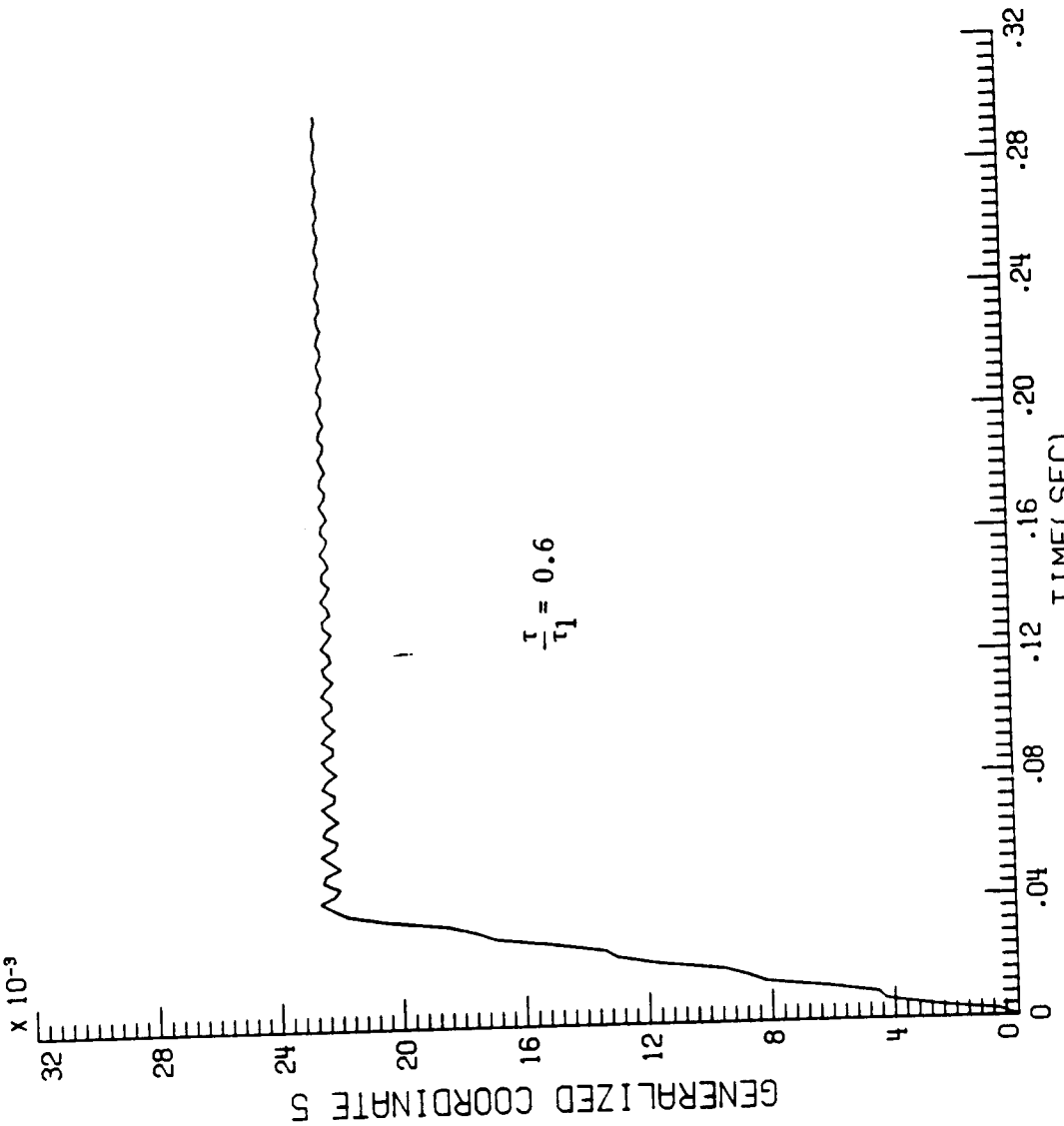

Figure 7e. - Mode 5 Generalized Coordinate for Ramp/Step Function.

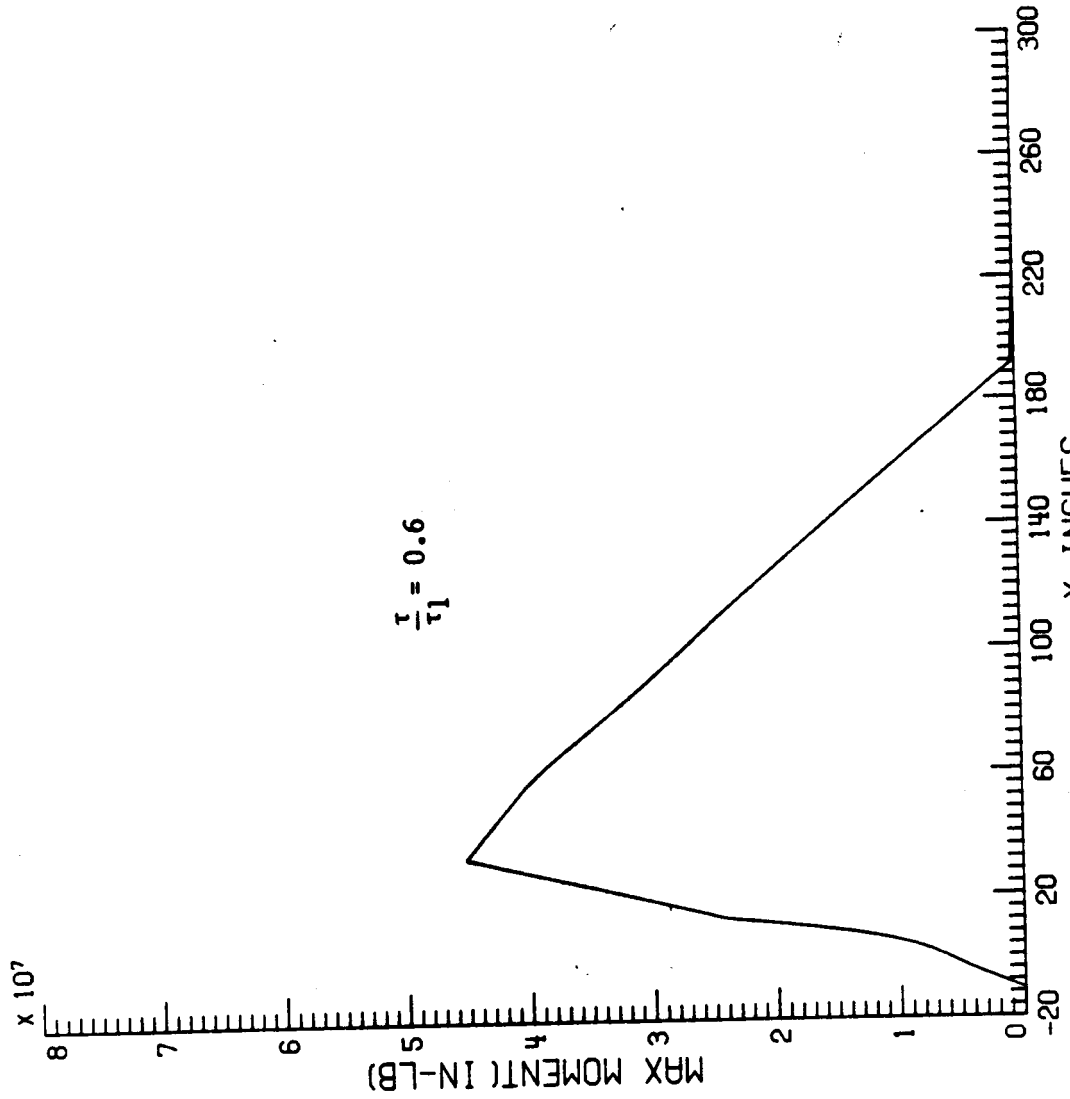

Figure 8. - Maximum Moment at Forward Bearing for Ramp/Step Function.

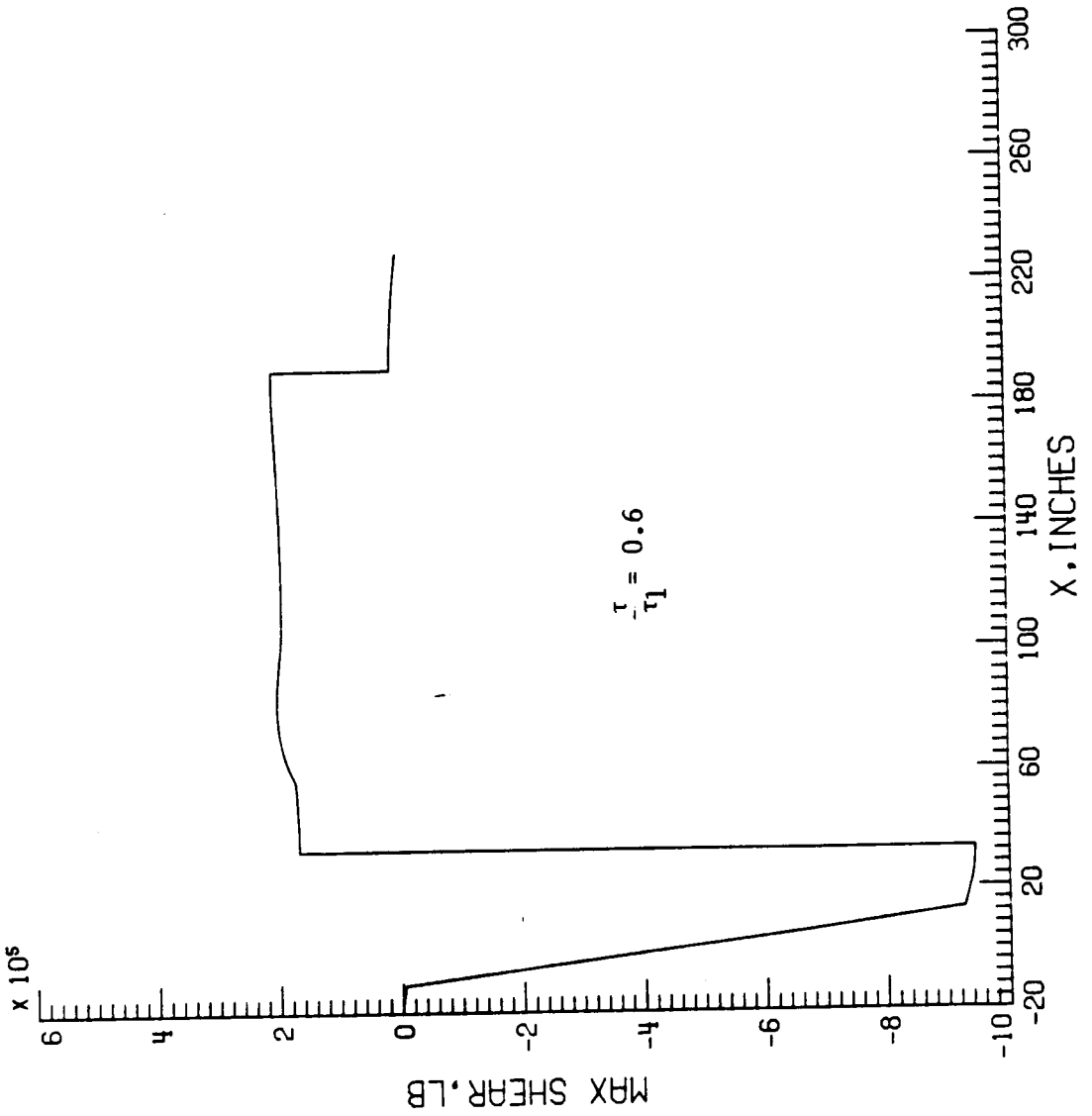

Figure 9. - Maximum Shear at Forward Bearing for Ramp/Step Function.

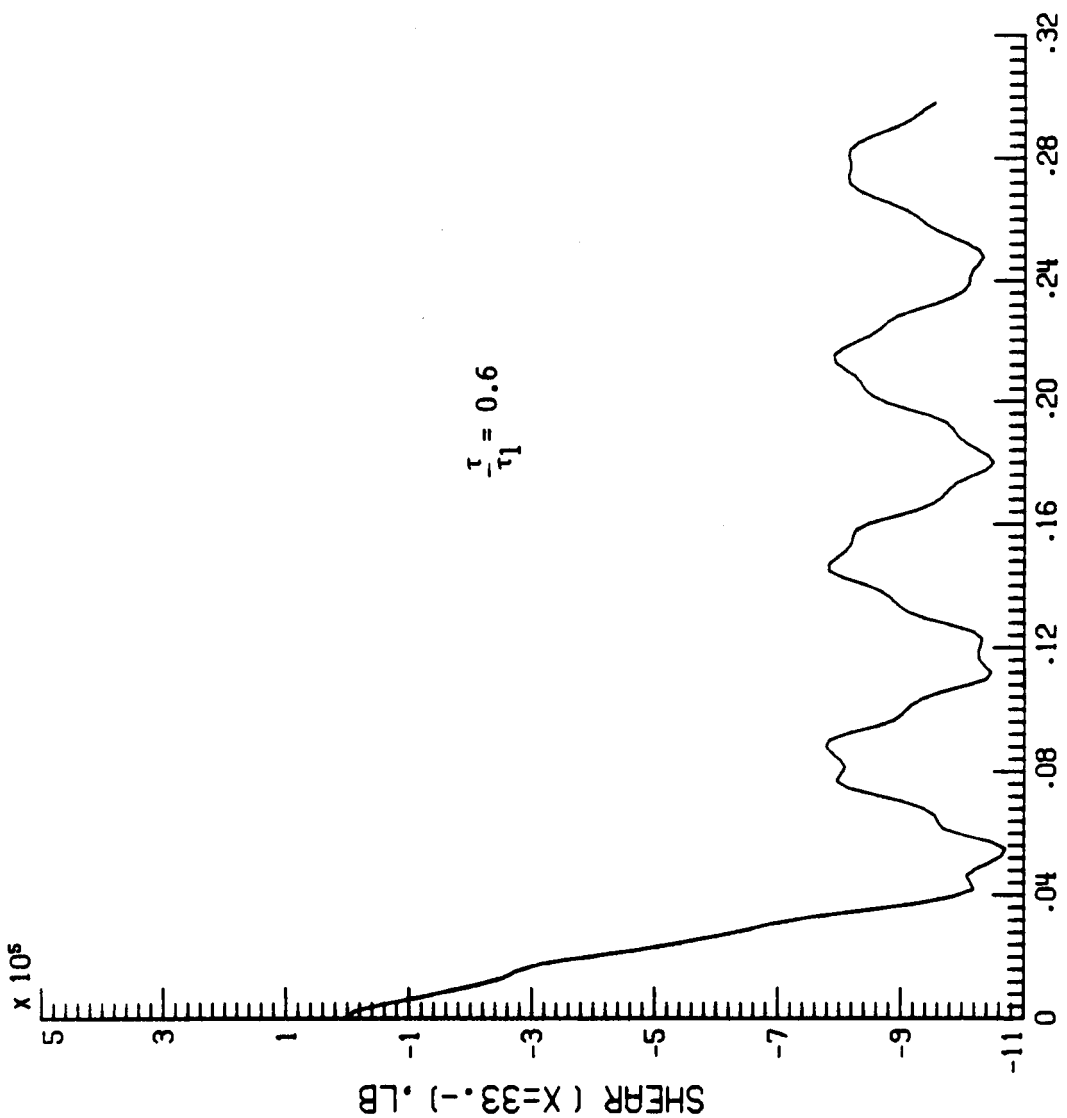

Figure 10a. - Ramp/Step Shear at Forward Bearing.

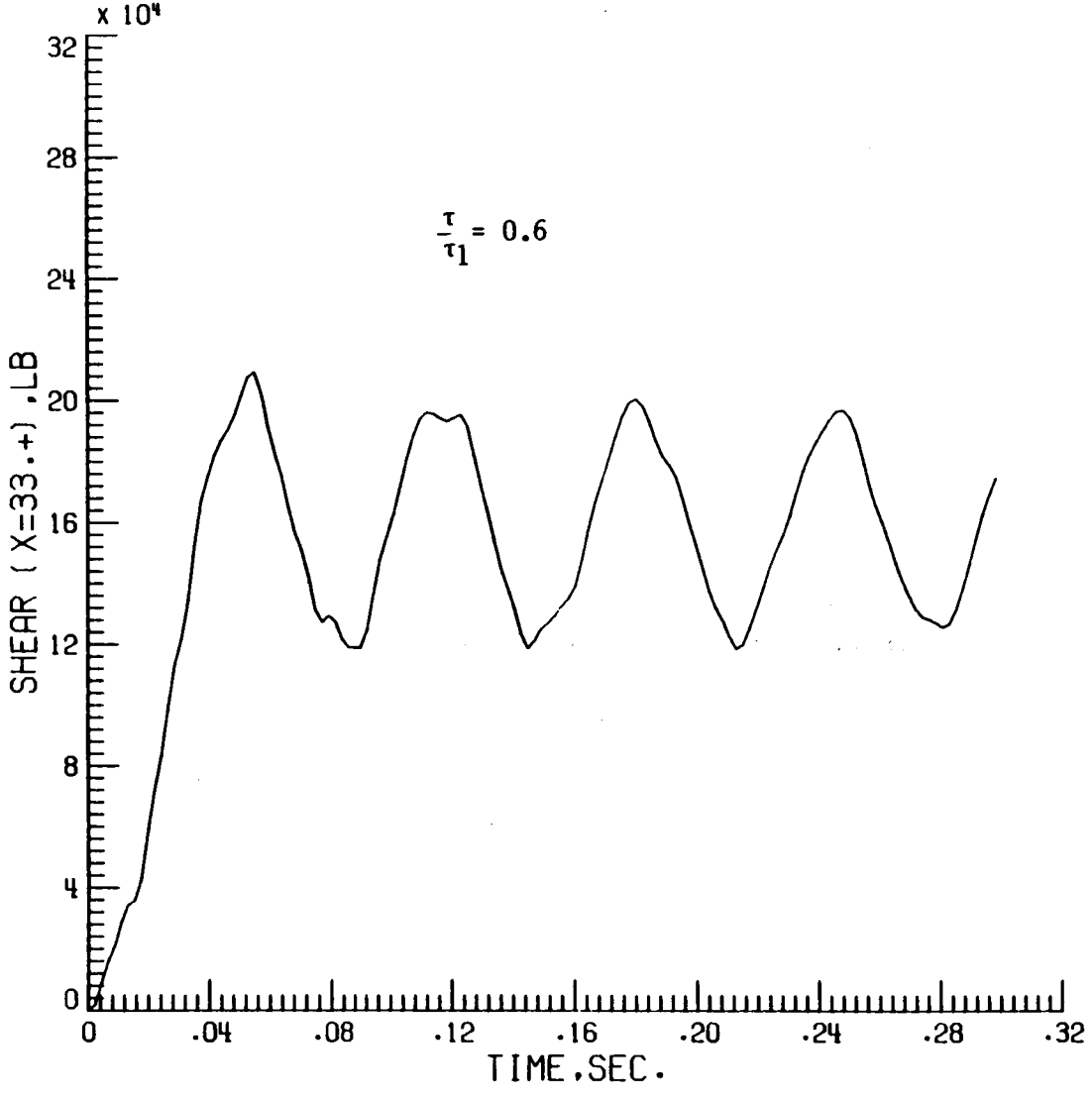

Figure 10b. - Ramp/Step Function Shear at Forward Bearing.

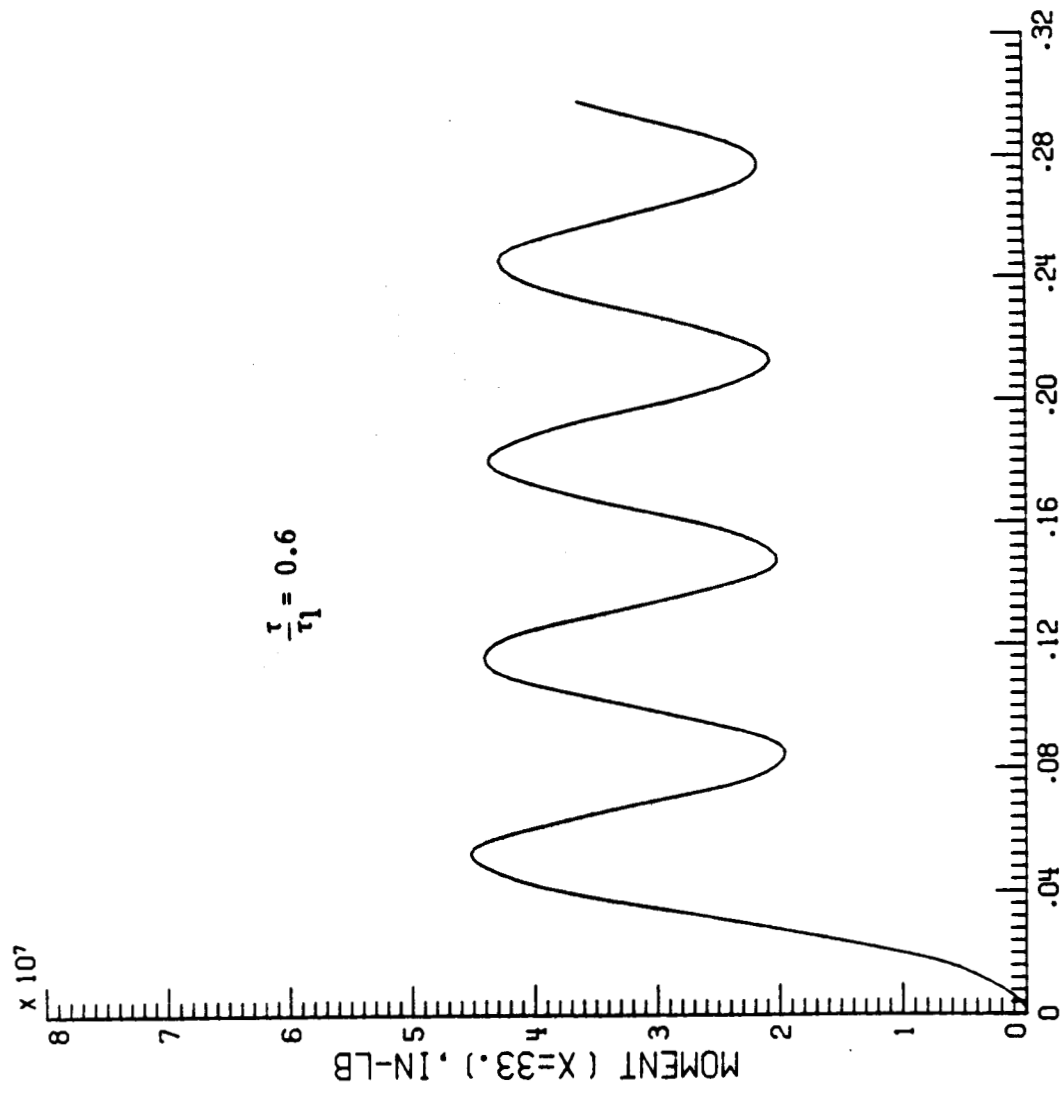

Figure 11. - Ramp/Step Moment at Forward Bearing.

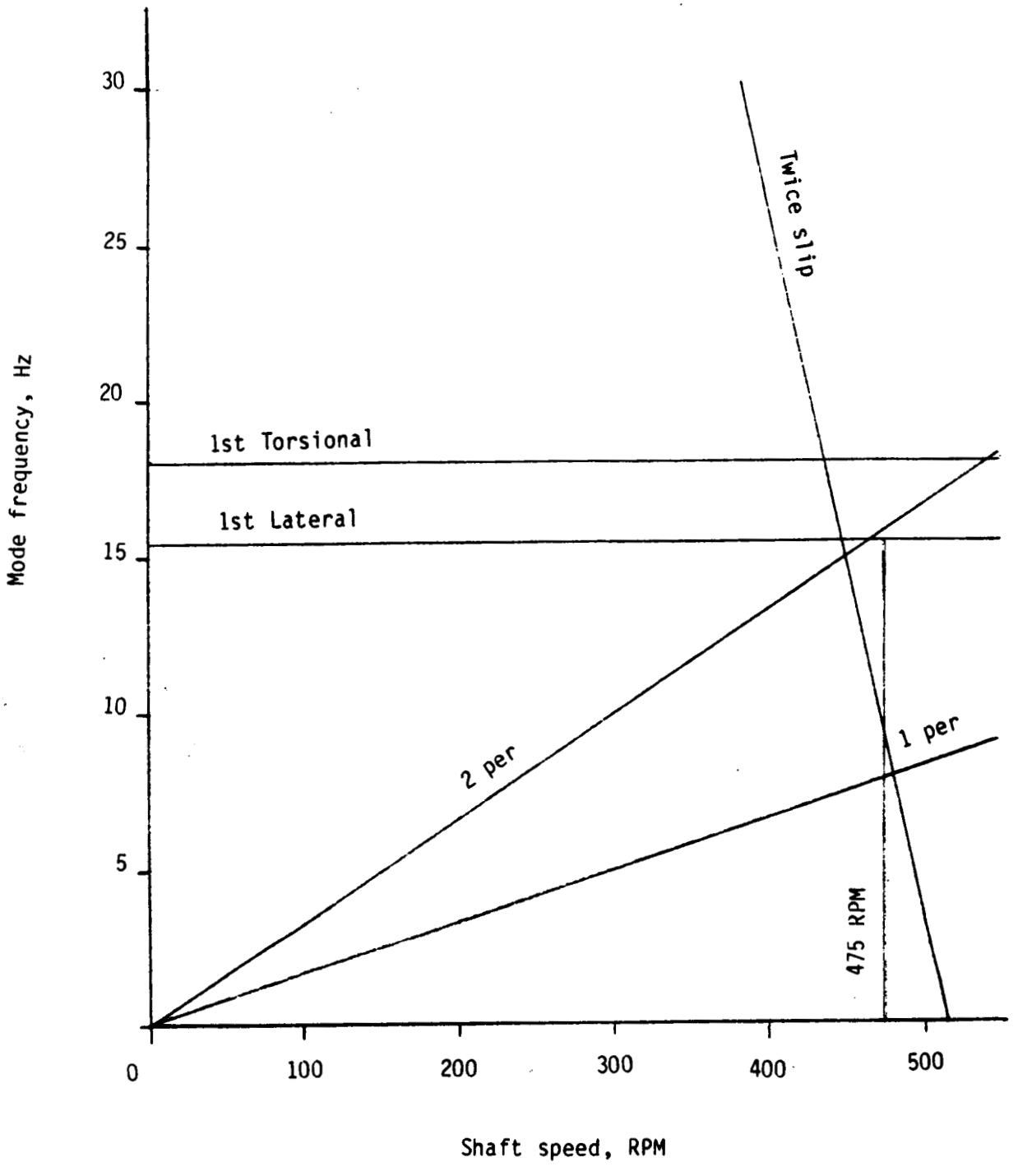

Figure 12. - Campbell Diagram for 7 X 10 Tunnel.

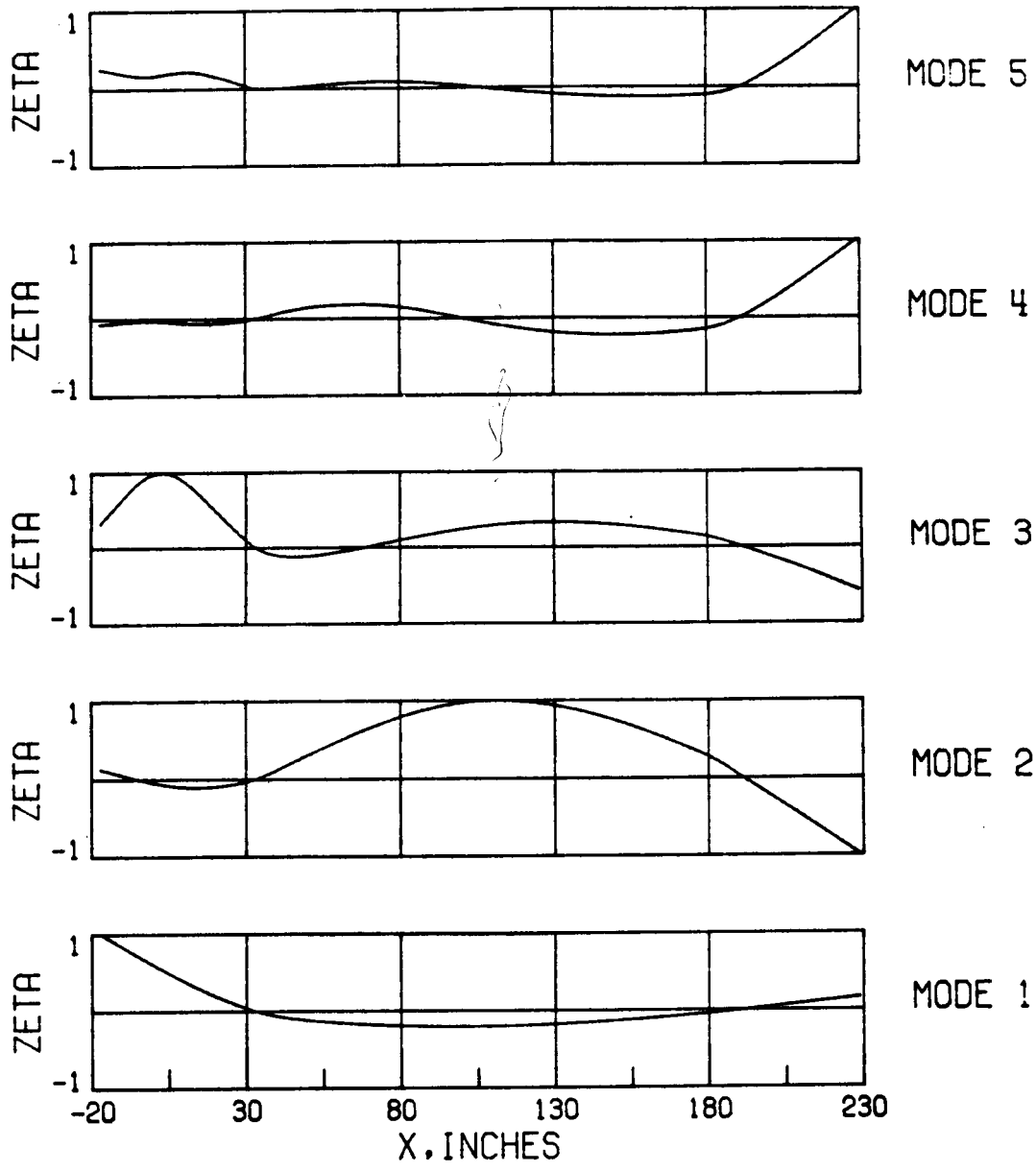

Figure 13. - 7 X 10 Drive System Lateral Mode Shapes.

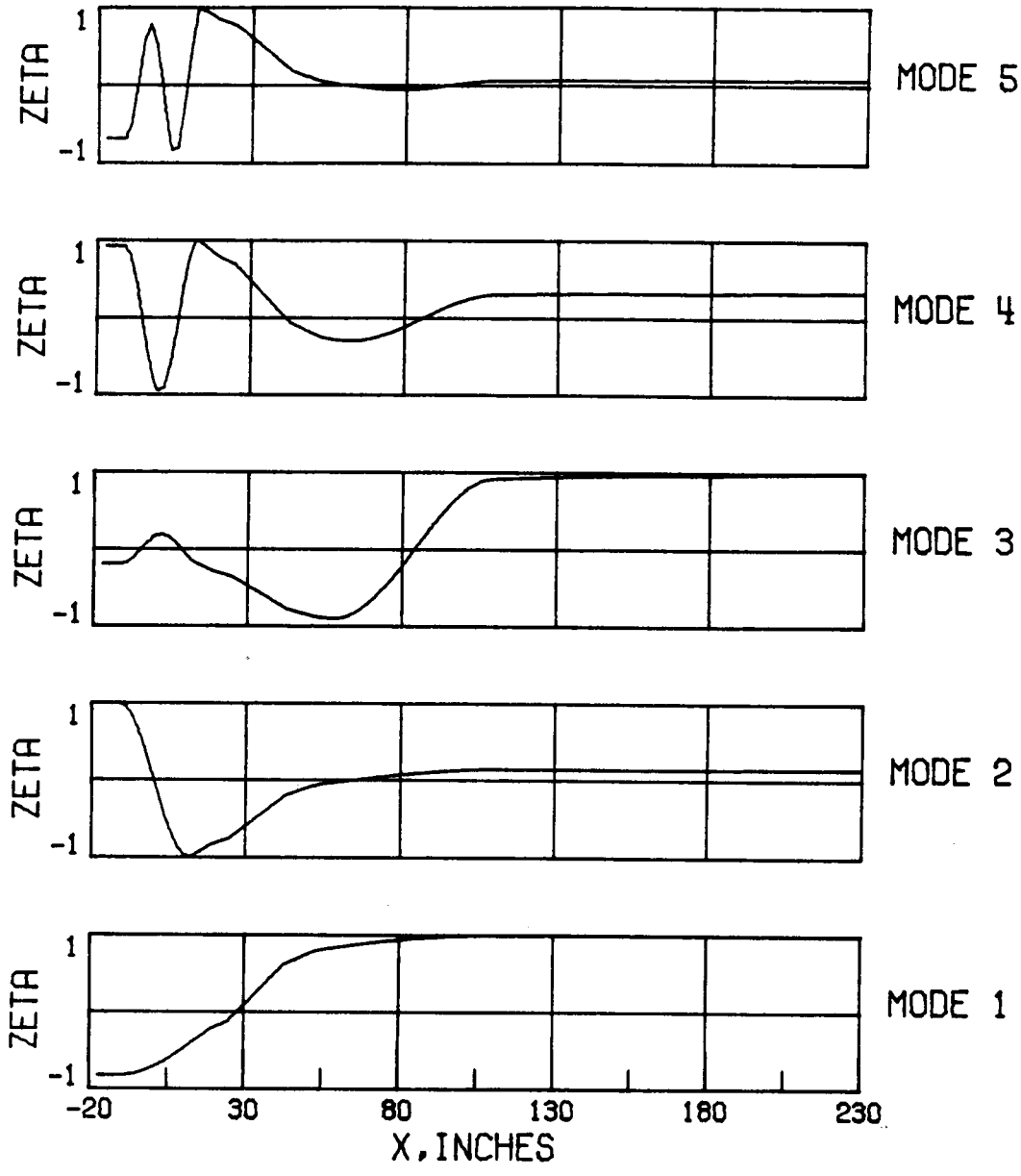

Figure 14. - 7 X 10 Drive System Torsional Mode Shapes.

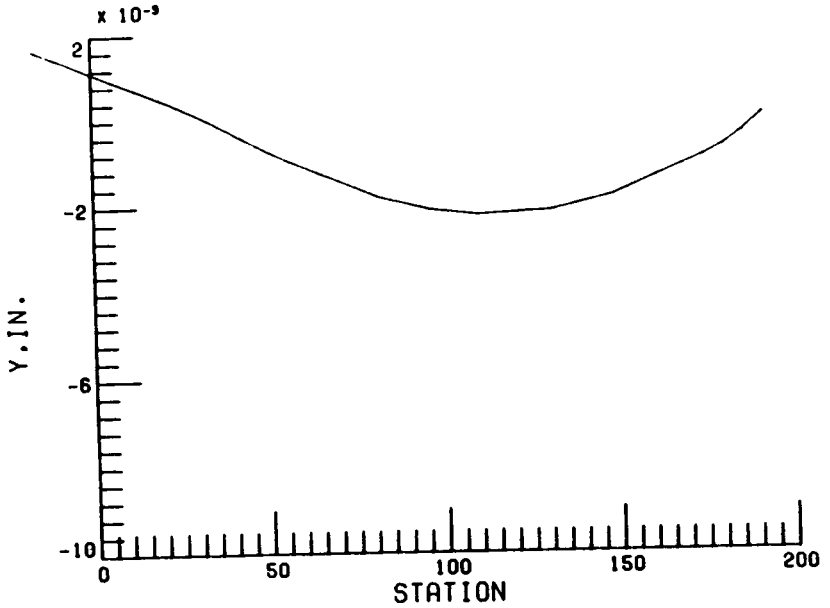

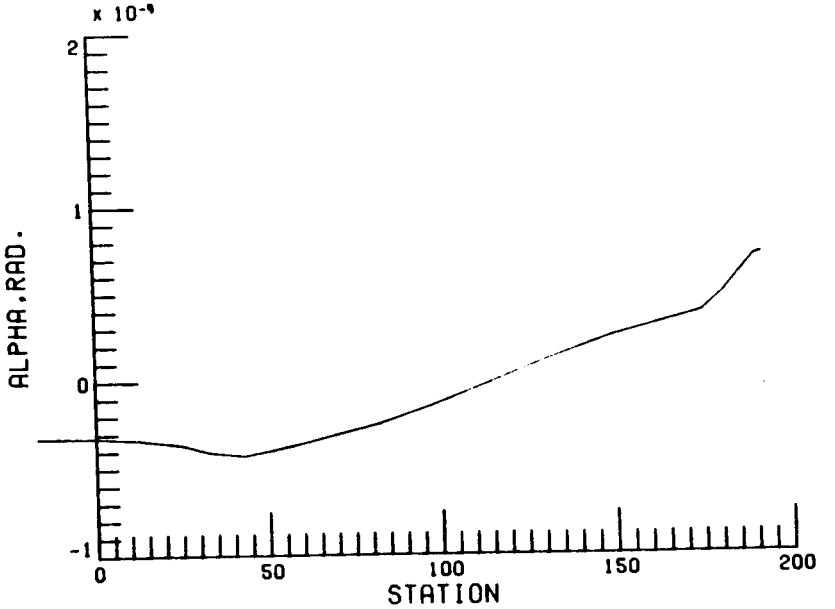

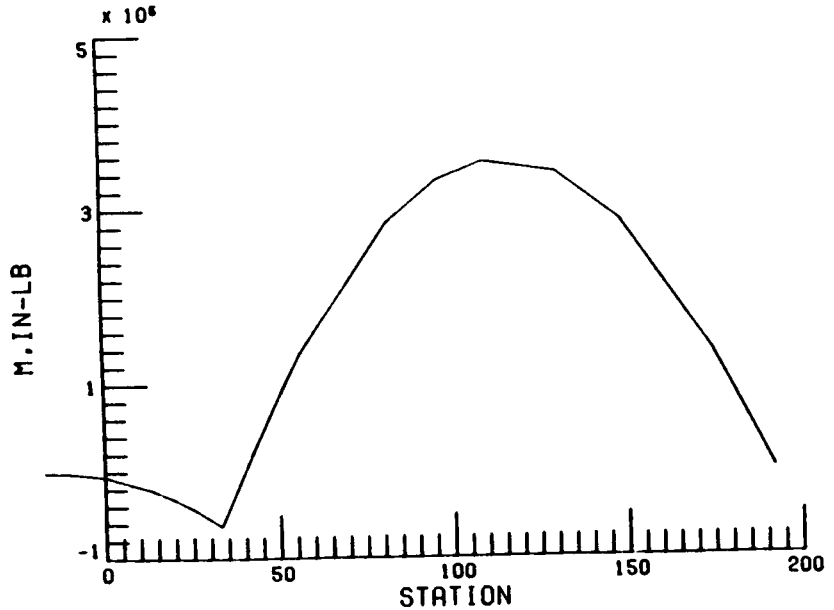

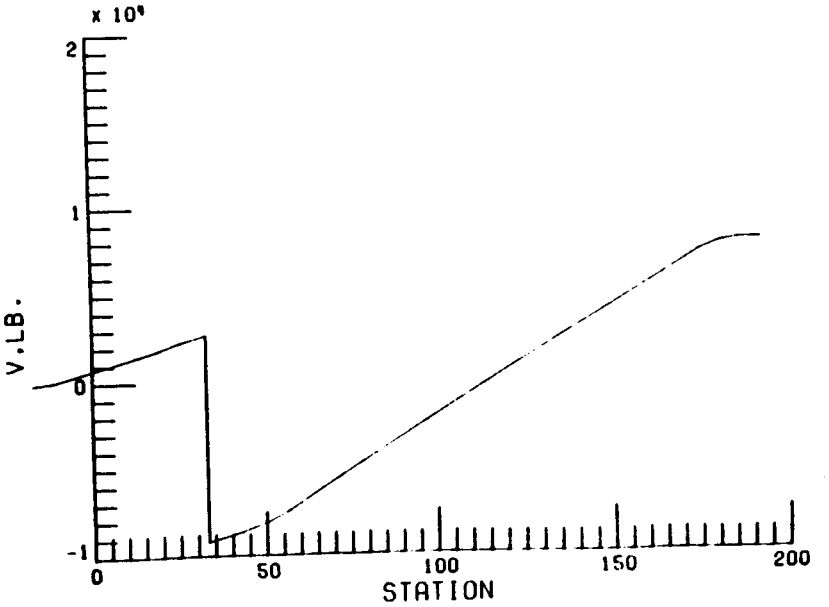

Figure 15. - Gravity Static Load Case for 7 X 10 Tunnel.

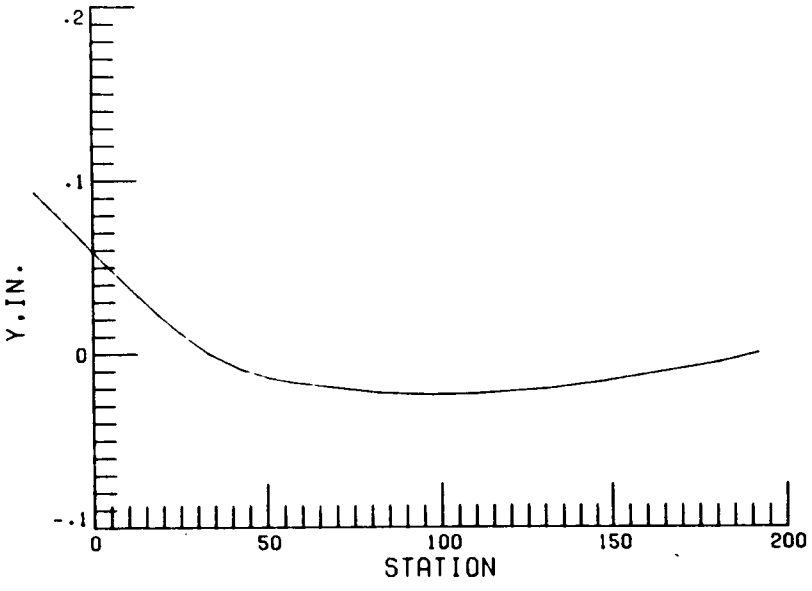

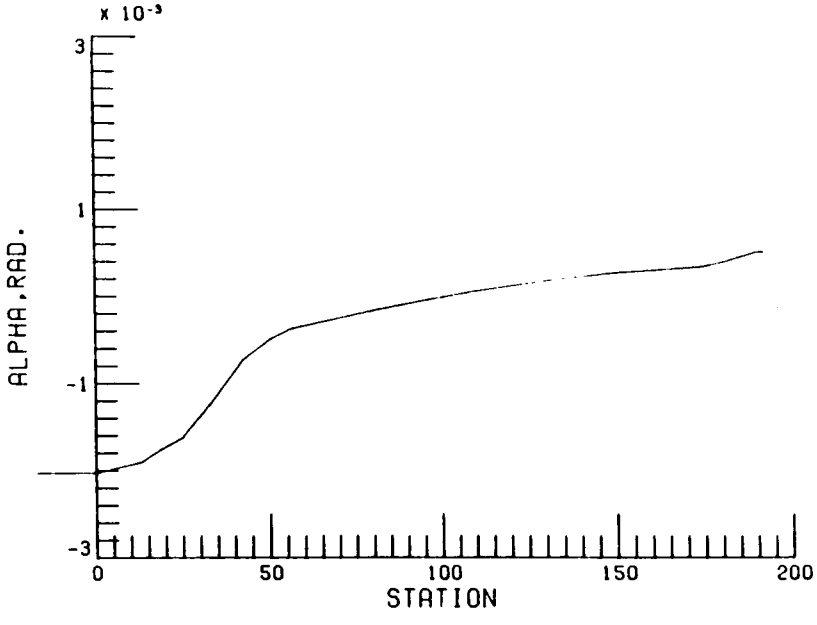

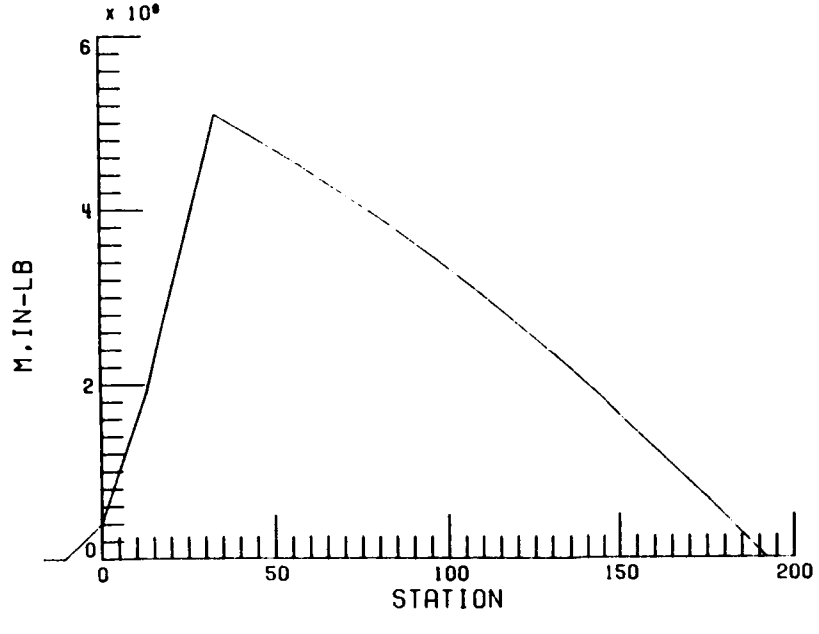

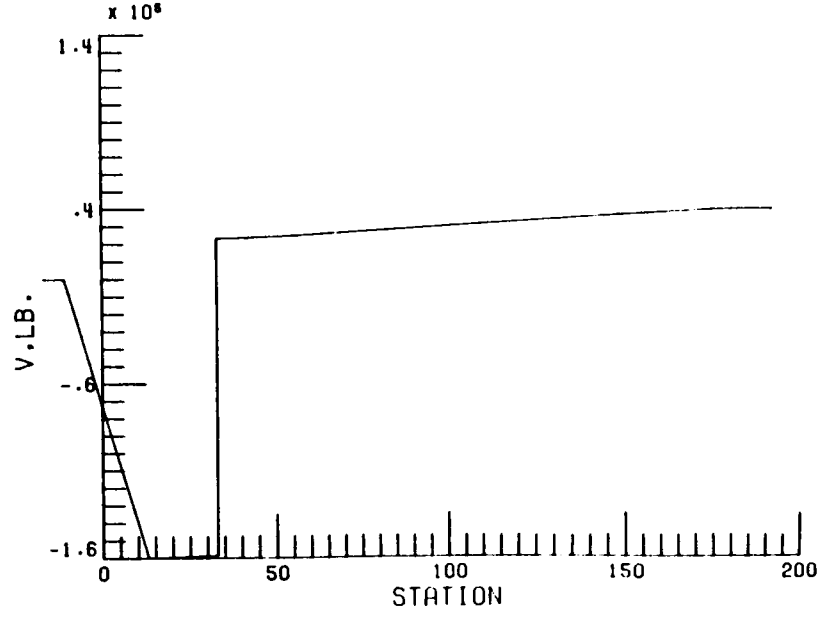

Figure 16. - Static Case - Force of 1 Blade Loss (1.6122E5 lb.).

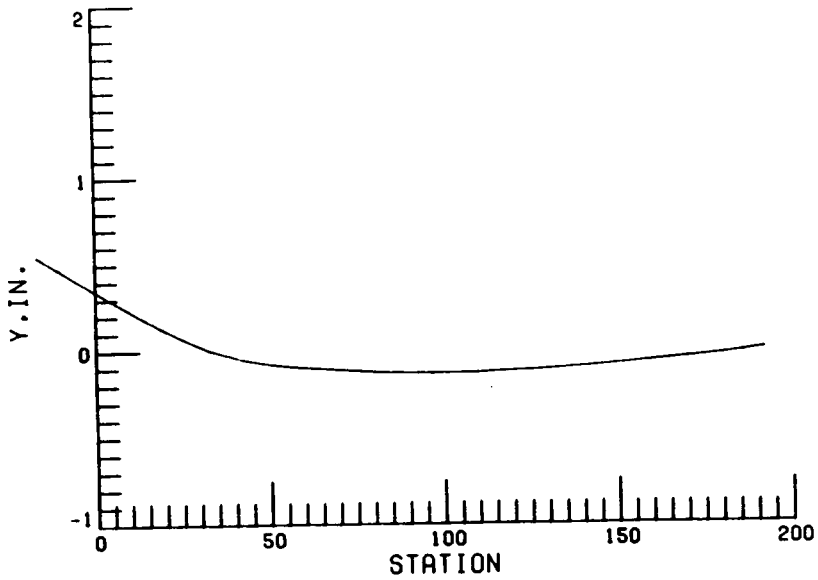

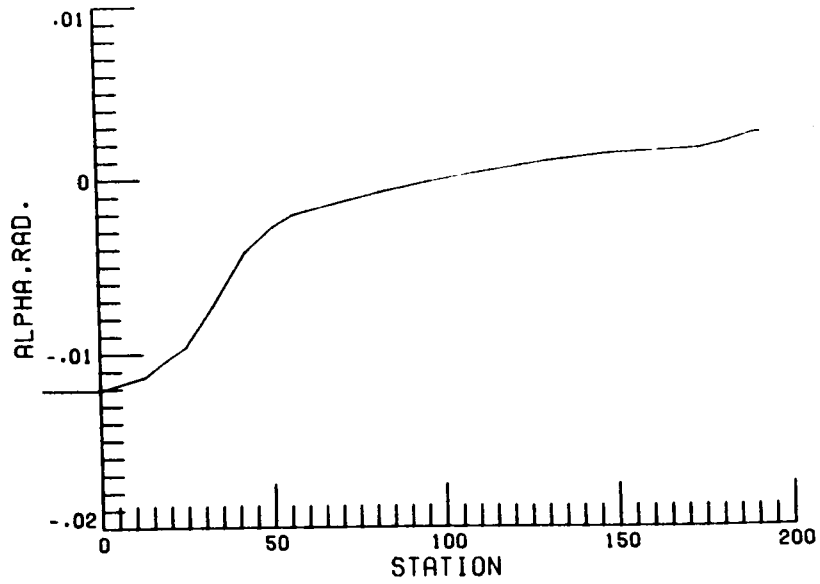

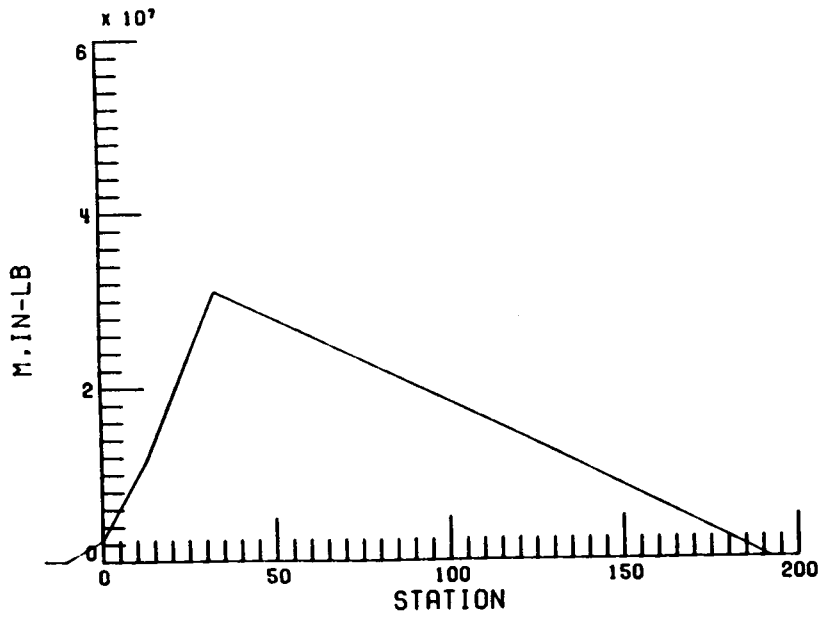

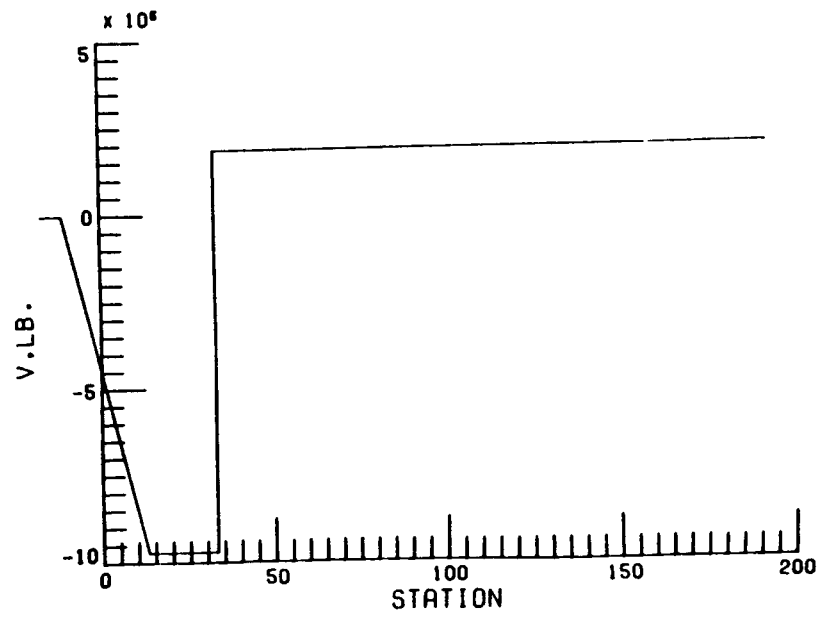

Figure 17. - Static Case - Force of 9 Blades Loss (9.283E5 lb.).

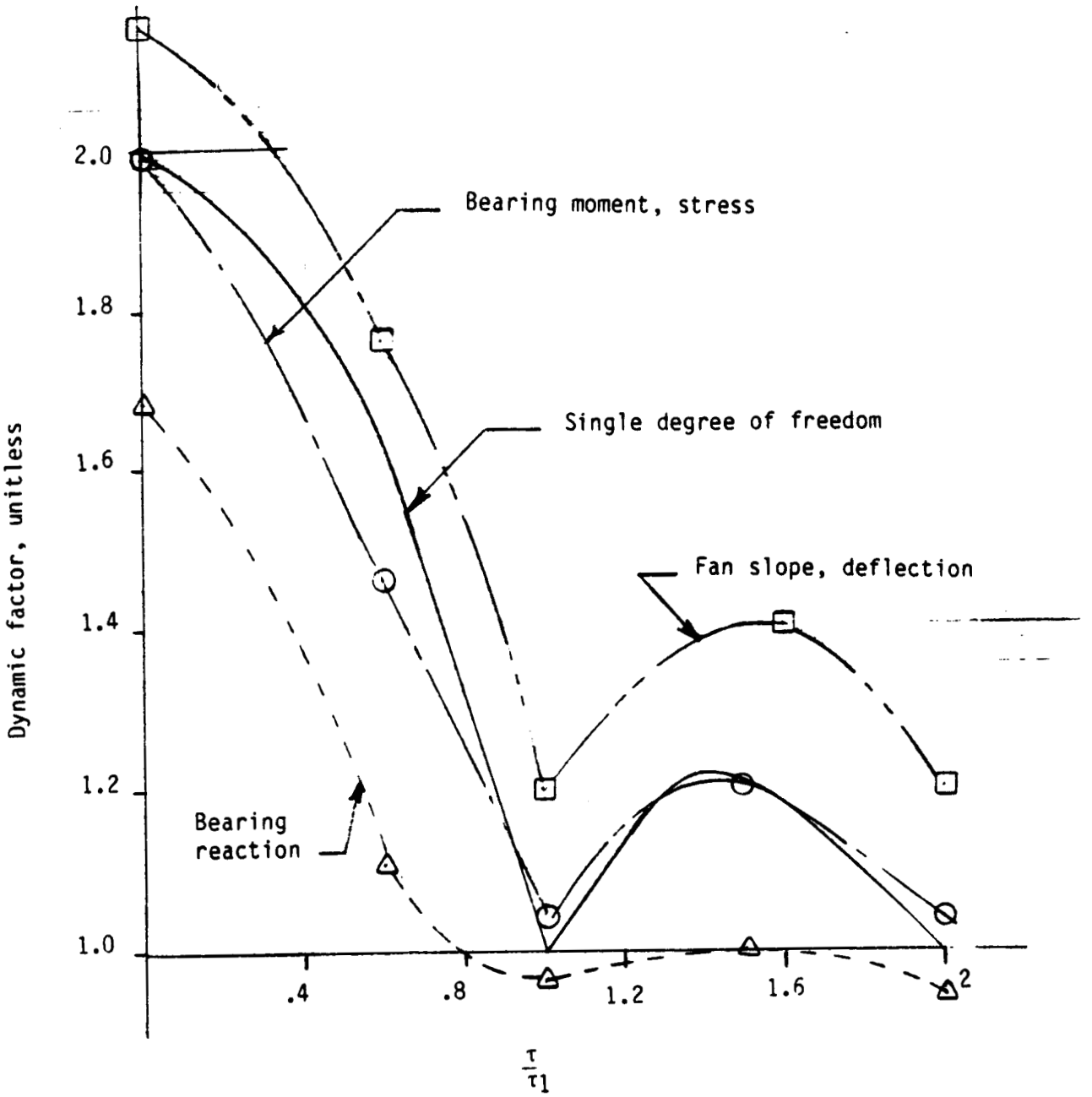

Figure 18. - Dynamic Factor as a Function of Rise Time.

Standard Bibliographic Page

1. Report No.	2. Government Accession No.	3. Recipient's Catalog No.
NASA TM-100504		

4. Title and Subtitle	5. Report Date
Analysis of 7- X 10-Foot High Speed Wind Tunnel Shaft Loads in Support of Fan Blade Failure Investigation	November 1987
	6. Performing Organization Code
7. Author(s)	8. Performing Organization Report No.
Richard W. Faison	
9. Performing Organization Name and Address	10. Work Unit No.
NASA Langley Research Center Hampton, VA 23665-5225	505-61-01-07
	11. Contract or Grant No.
12. Sponsoring Agency Name and Address	13. Type of Report and Period Covered
National Aeronautics and Space Administration Washington, DC 20546	Technical Memorandum
	14. Sponsoring Agency Code

15. Supplementary Notes

16. Abstract

This report was accomplished to aid in the failure investigation of the High-Speed 7-x 10-Foot Wind Tunnel. The High-Speed 7-x 10-Foot Wind Tunnel at Langley Research Center, Hampton, Virginia, experienced a catastrophic failure of all 18 Sitka spruce fan blades during operation at 0.8 Mach number on July 2, 1985. The High-Speed Tunnel, a closed-circuit/single-return atmospheric wind tunnel, has been operated since 1945 to support a wide range of subsonic aerodyanmic tests and studies. The failed blade set had been in use since 1975. In addition to blade loss, the most significant damage was a bent main drive shaft for a total estimated damage loss of $1.7 million.

An analysis of the natural frequency characteristics as well as loads, reactions, stresses and deflections of the fan drive system resulting from steady-state and dynamic loads due to unbalance was performed. Transient load cases were simulated by step input and ramp input loading functions intended to simulate the loss of one to nine blades (maximum unbalance forces).

17. Key Words (Suggested by Authors(s))	18. Distribution Statement
Drive shaft dynamic response Shaft stresses Dynamics of blade loss Dynamic system response to fan blade failure	Unclassified - Unlimited Subject Category 09

19. Security Classif.(of this report)	20. Security Classif.(of this page)	21. No. of Pages	22. Price
Unclassified	Unclassified	48	A03

For sale by the National Technical Information Service, Springfield, Virginia 22161